Mutations of the YidC Insertase alleviate stress from σ^M-dependent membrane protein overproduction in *Bacillus subtilis*

Short Title: Gain of function mutations in the YidC membrane insertase

Heng Zhao[1#a], Ankita J. Sachla[1], and John D. Helmann[1]*

[1] Department of Microbiology, Cornell University, Ithaca, NY, USA 14853-8101

[#a] Current Address: Department of Microbial Pathogenesis, Yale University School of Medicine, New Haven, Connecticut, USA.

* Corresponding author

E-mail: jdh9@cornell.edu (JDH)

Co-author emails: *hz285@cornell.edu, ajs588@cornell.edu*

Abstract

In *Bacillus subtilis*, the extracytoplasmic function σ factor σ^M regulates cell wall synthesis and is critical for intrinsic resistance to cell wall targeting antibiotics. The anti-σ factors YhdL and YhdK form a complex that restricts the basal activity of σ^M, and the absence of YhdL leads to runaway expression of the σ^M regulon and cell death. Here, we report that this lethality can be suppressed by gain-of-function mutations in *spoIIIJ*, which encodes the major YidC membrane protein insertase in *B. subtilis*. *B. subtilis* PY79 SpoIIIJ contains a single amino acid substitution in the substrate-binding channel (Q140K), and this allele suppresses the lethality of high SigM. Analysis of a library of YidC variants reveals that increased charge (+2 or +3) in the substrate-binding channel can compensate for high expression of the σ^M regulon. Derepression of the σ^M regulon induces secretion stress, oxidative stress and DNA damage responses, all of which can be alleviated by the $YidC^{Q140K}$ substitution. We further show that the fitness defect caused by high σ^M activity is exacerbated in the absence of SecDF protein translocase or σ^M-dependent induction of the Spx oxidative stress regulon. Conversely, cell growth is improved by mutation of specific σ^M-dependent promoters controlling operons encoding integral membrane proteins. Collectively, these results reveal how the σ^M regulon has evolved to up-regulate membrane-localized complexes involved in cell wall synthesis, and to simultaneously counter the resulting stresses imposed by regulon induction.

Author Summary

Bacteria frequently produce antibiotics that inhibit the growth of competitors, and many naturally occurring antibiotics target cell wall synthesis. In *Bacillus subtilis*, the alternative σ factor σ^M is induced by cell wall antibiotics, and upregulates genes for peptidoglycan and cell envelope

43 synthesis. However, dysregulation of the σ^M regulon, resulting from loss of the YhdL anti-σ^M
44 protein, is lethal. We here identify charge variants of the SpoIIIJ(YidC) membrane protein
45 insertase that suppress the lethal effects of high σ^M activity. Further analyses reveal that induction
46 of the σ^M regulon leads to high level expression of membrane proteins that trigger envelope stress,
47 and this stress is countered by specific genes in the σ^M regulon.
48

49 ## Introduction

50 The ability of cells to adapt to changing conditions relies in large part on the expression of
51 specific stress responses controlled by transcription regulators. The extracytoplasmic function
52 (ECF) subfamily of σ factors are frequently involved in bacterial responses to stresses affecting
53 the cell envelope [1, 2]. In *Bacillus subtilis*, there are seven ECF σ factors with the σ^M regulon
54 playing a particularly important role in modulating pathways involved in peptidoglycan synthesis,
55 cell envelope stress responses, and intrinsic resistance to antibiotics [3]. Cells lacking σ^M (*sigM*
56 null mutants) grow normally in unstressed conditions, but have greatly increased sensitivity to
57 high salt and to cell wall active antibiotics, including ß-lactams and moenomycin [4-6].

58 Like many other ECF σ factors, the activity of σ^M is regulated by two membrane-localized
59 anti-σ factors encoded as part of the *sigM* operon, *sigM-yhdL-yhdK* [7, 8]. The major anti-σ factor
60 is YhdL, a transmembrane protein that directly binds σ^M [9]. However, full YhdL activity requires
61 a second transmembrane protein YhdK. Although a lack of σ^M is well tolerated under unstressed
62 conditions, the lack of the anti-σ^M factors leads to a runaway activation of the autoregulated *sigM*
63 operon, and overexpression of the σ^M regulon [10]. A null mutation of *yhdK* leads to an ~100-fold
64 elevation of σ^M activity, morphological abnormalities, and slow growth [10]. A null mutation in
65 *yhdL* is lethal, but suppressors arise readily that have inactivated *sigM* and grow normally in

unstressed conditions [4, 10]. These findings imply that high level expression of σ^M is toxic to cells, but the basis for this toxicity has not been defined.

Previously, we explored the basis for σ^M toxicity by selecting for suppression of *yhdL* lethality in a *sigM* merodiploid strain to reduce the frequency of suppressors that had inactivated σ^M. These studies led to the recovery of mutations in *rpoB* and *rpoC*, encoding the ß and ß' subunits of RNA polymerase, that led to a reduction of σ^M activity sufficient to restore viability [10]. These mutations, which acted selectively on σ^M, affected a region of core RNA polymerase involved in σ factor binding. In the course of these studies we also demonstrated that the toxicity from high σ^M could be alleviated by mutation of the autoregulatory promoter for the *sigM* operon, or by overexpression of the housekeeping σ factor, σ^A [10]. These results suggest that the lack of a functional anti-σ^M factor (*yhdL* null mutant) leads to runaway activation of the *sigM* operon and a high level of σ^M activity that is incompatible with growth. However, it is unclear whether σ^M toxicity results from a decrease in activity of the essential housekeeping σ^A, overexpression of one or more σ^M-regulated genes, or both.

To further explore the impact of overexpression of specific σ^M-regulated genes on cell physiology we generated a library of strains in which specific σ^M-dependent promoters (P_M) are inactivated by point mutations. This approach, which removes σ^M-dependent activation while leaving other promoters and regulatory inputs intact, is important since many σ^M-regulated genes have multiple promoters and encode essential genes, including several involved in peptidoglycan synthesis and cell division [3]. In the course of developing this library we received a previously described strain with a mutation inactivating the P_M of *rodA*, encoding a SEDS family transglycosylase important for peptidoglycan synthesis [6]. We unexpectedly discovered that in this strain *yhdL* could be inactivated, and the same was true for the parent strain (*B. subtilis* PY79).

These serendipitous observations led us to hypothesize that *B. subtilis* PY79 differs from other *B. subtilis* 168 strains in its ability to tolerate high level expression of the σ^M regulon.

Here, we report that the ability of *B. subtilis* PY79 to tolerate σ^M regulon overexpression results from a single amino acid substitution in the *spoIIIJ* gene, which encodes the major YidC membrane insertase in *B. subtilis* [11, 12]. This finding motivated a detailed structure-function analysis of YidC, which led to the discovery of mutations that increase the positive charge within the hydrophilic, substrate-binding channel of YidC from +1 (wild-type) to +2 or +3 (in specific combinations) increase tolerance to overexpression of σ^M-regulated membrane proteins. Moreover, high level activity of σ^M leads to induction of genes associated with secretion stress, oxidative stress, and DNA damage responses, and the σ^M regulon itself includes functions that help compensate for stresses associated with membrane protein overexpression.

Results

A single amino acid change in SpoIIIJ necessary and sufficient for tolerance of high σ^M

The anti-σ factors YhdL and YhdK regulate σ^M, and the absence of *yhdL* is lethal in *B. subtilis* strain 168 due to toxic levels of σ^M [4, 10]. Since σ^M controls a large regulon, including many essential genes involved in cell wall synthesis [1, 3], we sought to construct a library of strains in which specific σ^M-dependent promoters are inactivated by point mutations. One such promoter precedes *rodA*, which encodes a peptidoglycan transglycosylase [6]. We thus acquired a ΔP_M-*rodA* strain (BAM1077[6]), and tested whether *yhdL* is essential in that strain background, with its parent wild type strain PY79 as a control. Surprisingly, we found that *yhdL* is not essential in either PY79 strain. A *yhdL* mutant in PY79 exhibits reduced colony size compared to WT and high σ^M activity as indicated by the blue color on LB plates containing X-Gal (Fig. 1a). This mutant

112 is relatively stable, with the occasional appearance of suppressors that have a large white colony
113 morphology (likely containing mutations in *sigM*). In contrast, introduction of a *yhdL* null mutation
114 into other *B. subtilis* 168 strains results in tiny, pinpoint colonies that cannot be re-streaked,
115 consistent with prior work [4, 10].

116 To identify the genetic differences in PY79 that confer tolerance of high σ^M, we compared
117 the genome between *B. subtilis* strain 168 and PY79. There are over a hundred single nucleotide
118 polymorphisms (SNPs) between the 168 reference sequence and PY79, as well as four large
119 deletions in the genome of PY79 (including the SPβ prophage), causing a reduction of 180 kb for
120 the PY79 genome compared with 168 [13, 14]. To identify differences that might correlate with
121 tolerance of high σ^M activity, we compared the sequences of genes encoding RNA polymerase
122 subunits, and genes in the σ^M and Spx regulons (Spx is a transcription regulator that is regulated
123 by σ^M). However, no differences were noted in these 103 genes between the PY79 and 168
124 reference genomes (Table S1).

125 Next, we used an unbiased, forward genetics approach to identity the mutation in PY79
126 that suppresses the lethality of a *yhdL* null mutation. We used genomic DNA from a PY79
127 *yhdL*::*kan* strain to transform 168 to kanamycin resistance, reasoning that the only viable
128 transformants will likely also acquire the suppressing mutation. Because each competent cell of *B.*
129 *subtilis* contains about 50 binding sites for DNA uptake, a competent cell can import multiple
130 fragments of DNA during transformation in a process known as congression [15]. When a 168
131 strain containing a P_M-*lacZ* reporter was transformed with chromosomal DNA from the viable
132 PY79 *yhdL*::*kan* strain and selected on an LB plate supplemented with kanamycin and X-gal, we
133 recovered numerous tiny blue colonies that did not grow when re-streaked onto fresh plates
134 (consistent with the essentiality of YhdL in the 168 background), a few large white colonies (likely

sigM mutants), and intermediate sized blue colonies (Fig. 1B). The intermediate blue colonies grew to a similar size as a *yhdL* null mutant in PY79, consistent with acquisition of both the *yhdL*::*kan* allele and a second locus that suppresses the toxicity of high σ^M. Whole genome sequencing was performed on these transformants and the reads were mapped to the reference genome of 168. Out of 15 sequenced 168 transformants, 14 contained the same SNP imported from PY79 that generates a missense mutation in *spoIIIJ* (encoding SpoIIIJ^{Q140K}) (Fig. S1A, Table S2). We therefore hypothesized that the *spoIIIJ*^{Q140K} allele was the suppressor needed for cells to tolerate the *yhdL* mutation.

SpoIIIJ belongs to the YidC membrane protein insertase family and is responsible for inserting membrane proteins into the lipid bilayer, independently or in association with the Sec secretion system [16-18]. *E. coli* encodes one essential homolog of YidC, while some bacteria such as *B. subtilis* encode two homologs, SpoIIIJ(YidC) and YidC2 [18, 19]. The gene encoding YidC was named *spoIIIJ* because mutations at this locus lead to a block at stage III of sporulation [19, 20]. However, *spoIIIJ* is constitutively expressed and functional in vegetative cells. The expression of the paralog YidC2 is regulated by an upstream gene *mifM*, which monitors the total membrane protein insertase activity and only allows expression of YidC2 when MifM is not efficiently inserted into the membrane [21]. Both SpoIIIJ and YidC2 can fulfill the essential function of YidC insertase, with SpoIIIJ essential for sporulation [22] and YidC2 important for the development of competence (Fig. S2A) [23]. Interestingly, an alignment of YidC homologs revealed that the Gln140 residue is highly conserved among bacteria, and only *B. subtilis* PY79 SpoIIIJ contains Lys at this position (Fig. 1C).

To test if this SpoIIIJ Gln to Lys variant (SpoIIIJ^{Q140K}) is necessary and sufficient for tolerance of high σ^M, we introduced the *spoIIIJ*^{Q140K} mutation at the native locus of strain 168 using

158 CRISPR, and found that *yhdL* was no longer essential (Fig. 1D, Fig. S1B). Conversely, changing
159 the Lys140 into Gln in PY79 abolished the ability of PY79 to tolerate loss of *yhdL* (Fig. S1B),
160 suggesting that the SpoIIIJ^{Q140K} is necessary and sufficient for tolerance of a *yhdL* deletion
161 mutation. To test if the *spoIIIJ*^{K140} allele is dominant over the *spoIIIJ*^{Q140} allele, we constructed
162 merodiploid strains expressing both alleles of SpoIIIJ (using a vector with xylose-inducible
163 promoter P_{xylA} that integrates into *ganA* and when induced produces about 70% amount of the
164 native protein level (Fig. 2B)). Strains with either a P_{xylA}-*spoIIIJ*^{K140} in the 168 strain, or P_{xylA}-
165 *spoIIIJ*^{Q140} in PY79 strain background could still tolerate the loss of *yhdL* (Fig. S1B). This
166 dominance suggests that SpoIIIJ^{Q140K} leads to a gain of function that enables cells to tolerate high
167 σ^M activity. Phase contrast microscopy revealed that a 168 SpoIIIJ^{Q140K} *yhdL* mutant had a similar
168 but slightly more elongated cell morphology compared with a PY79 *yhdL* mutant (Fig. 1E),
169 confirming the major role of SpoIIIJ^{Q140K} in tolerance of a *yhdL* null mutation.

170 As a general strategy to monitor cell fitness, we compared the impact of *spoIIIJ* alleles on
171 morphology and colony size in the PY79 and 168 backgrounds mutant for *yhdK*. YhdK functions
172 together with YhdL as an anti-σ complex, but unlike *yhdL* a *yhdK* null mutant is tolerated in 168
173 strains, although it does lead to an ~100-fold increase in σ^M regulon expression and severe growth
174 defects [10]. Five independent trials with a 168 *yhdK* mutant, known to generate small colonies,
175 revealed up to a ~10% change in average colony area. This variation likely results from small
176 differences in the plating conditions. Although these small differences were in some cases judged
177 to be statistically significant (based on P value in a t test, two tails, assuming unequal variances)
178 (Fig. S1C), this reflects the high sample number in each measurement (100-1000 colonies per
179 measurement). Considering this level of variation between genetically identical strains, we only
180 regard as significant those changes of >10% in colony size. Using this assay, we found that the

small colony size, as well as the filamentous cell morphology of the 168 *yhdK* mutant, can be largely rescued by the *spoIIIJ*^{Q140K} allele (Fig. 1F, G). Conversely, a *spoIIIJ*^{K140Q} mutation in PY79 *yhdK* converted the large colonies of the parent strain into the small round morphology of the 168 *yhdK* strain, and the cells exhibited increased filamentation (Fig. 1F, G). Deletion of *spoIIIJ* in a PY79 *yhdK* mutant mimicked a SpoIIIJ^{K140Q} mutation (Fig. 1G), likely because the cells now rely on the other YidC paralog, YidC2, which contains a glutamine residue in the equivalent position (Fig. 1C) [19]. Overall, our results show that SpoIIIJ^{Q140K} mutation is necessary and sufficient for *B. subtilis* to tolerate high σ^M activity caused by the absence of the anti-σ factor YhdL or its partner protein YhdK.

Overexpression of SpoIIIJ increases tolerance of high σ^M activity

We hypothesized that the SpoIIIJ^{Q140K} protein may simply be more active or abundant in cells than the native protein. To test if increasing insertase activity is sufficient to alleviate toxicity associated with high σ^M, we overexpressed the wild-type 168 SpoIIIJ^{Q140} protein using a strong IPTG inducible promoter, $P_{spac(hy)}$ [24]. Induction of the $P_{spac(hy)}$-*spoIIIJ*^{Q140} allele led to a three-fold increase in the amount of SpoIIIJ protein compared with WT (Fig. 2B), and increased the colony size of a *yhdK* mutant by 68% (Fig. 2A). This increase is less than the effect of the *spoIIIJ*^{Q140K} allele at the native locus (which increased *yhdK* colony size by 134%), and consistently it only marginally increased the growth of a *yhdL* depletion strain under depletion condition (Fig. S2C). The increase in the fitness of the *yhdK* mutant supports the hypothesis that higher insertase activity is beneficial for cells with elevated σ^M activity, but overexpression alone does not phenocopy the effect of the altered function allele.

We next tested whether overexpression of YidC2, the other YidC homolog in *Bacillus*, could benefit cells with high σ^M expression. Interestingly, when *yidC2* was overexpressed from the $P_{spac(hy)}$ promoter, the growth defect of either the *yhdK* mutant or the *yhdL* depletion strain was exacerbated (Fig. 2A, S2C). Furthermore, when the equivalent glutamine residue of SpoIIIJ^{Q140} was mutated to lysine, the YidC2^{Q148K} mutant protein was toxic when overexpressed in a *yhdK* mutant (Fig. S2B). Thus, YidC2 is unable to compensate for SpoIIIJ in alleviating stress associated with high σ^M activity, even when the corresponding Gln to Lys substitution is present. Similarly, overexpression of *E. coli* YidC did not provide any benefit to a *yhdK* or *yhdL* mutant (Fig. 2A). However, when the equivalent Gln to Lys substitution was present, overexpression of the *E. coli* YidC^{Q429K} mutant was modestly beneficial, and colony size of the *yhdK* mutant increased by 58% (Fig. 2A). These results suggest that different YidC homologs vary in their substrate preferences, and the Gln to Lys mutation may enhance the ability of the *B. subtilis* SpoIIIJ and *E. coli* YidC insertases to facilitate membrane insertion of at least some σ^M-dependent proteins.

SpoIIIJ^{Q140K} increases the positive charge inside the substrate binding groove

The structure of YidC2 from *Bacillus halodurans* revealed a positively charged hydrophilic groove formed by five transmembrane segments [16]. A positively charged residue in the substrate-binding groove is essential for the function of the insertase, as a R73A substitution in *B. subtilis* SpoIIIJ completely abolished the essential function of SpoIIIJ *in vivo,* while an R73K substitution retained function [16]. Although the positive charge is essential, the R73 residue is not, as the positive charge can be provided by mutation of any of six other residues inside the hydrophilic groove to Arg. These six positions include Ile72 and Ile76 in transmembrane region 1 (TM1), Gln140 and Leu144 in TM2, and Trp228 and Gly231 in TM5 [25] (Fig. 3A, S3B). Since

both Arg and Lys are positively charged, we hypothesized that the key feature of the PY79 SpoIIIJ^{K140} protein is the +2 charge inside its substrate binding chamber. To test this hypothesis, we engineered a SpoIIIJ^{R73AQ140K} double substitution protein with a net charge of +1, where R73 is functionally replaced by K140. Expression of this protein is sufficient to support viability, as judged in a strain with depletion of *yidC2* (Fig. 3B), but is not sufficient to allow depletion of *yhdL* (Fig. 1D). This supports the idea that the key effect of the Q140K substitution is to increase the positive charge in the substrate binding groove.

Increased charge inside the substrate binding groove is key for tolerance of high σ^M activity

Since it is the increased positive charge from +1 to +2, rather than the Q140K substitution *per se*, that rescues cells from high σ^M toxicity, we next set out to test if other combinations of positively charged residues can also rescue cells from high σ^M activity. To this end, we generated a library of SpoIIIJ variants with five of the six positions mentioned above substituted (or not) with Arg, as shown previously to support function in the absence of Arg73 [25], and Gln140 substituted (or not) with Lys, as seen in PY79. In addition, we mutated Arg73 to Ala (or not) (Fig. 3A). This leads to 2^7=128 possible charge combinations, ranging from 0 to a maximum of +7, with most containing a nominal positive charge of +2 to +5 in the substrate binding groove (Fig. S3A, S3B). Note that for the sake of simplicity, we assume that the K140 residue is positively charged, since the epsilon-amino group of free Lys has a pKa of ~10.5, but this will likely vary depending on the local charge environment.

To identify SpoIIIJ variants that can function to support growth of a *yhdL* depletion strain, we transformed a *spoIIIJ* null *yhdL* depletion strain and selected for transformants that grew in the absence of *yhdL* induction. After sequencing and validation, we identified 103 *spoIIIJ* mutants that

supported growth in the absence of *yhdL* induction (Table S3). Among them, 88 mutants contained a nominal double positive charge in 13 unique combinations (Fig. S3A). Five of these 13 combinations include K140, including the combination present in the PY79 SpoIIIJ protein: R73 K140. The remaining 15 mutants contained a nominal triple positive charge, with four unique combinations. Interestingly, all four of these variants contained K140, and in each case K140 was present together with a pair Arg residues that also supported growth with Q140. It is possible that the presence of nearby Arg residues lowers the pKa of K140, and the protonation state of this residue may also vary depending on the nature of the bound substrate. Among the 17 unique combinations of double and triple positive charges, none has more than one positive charge in TM1, whereas TM2 and TM5 can each harbor double positive charges (Fig. S3A, Table S3). We conclude that all 17 functional SpoIIIJ variants have an effective charge of between +2 and +3 in the substrate binding channel. This strongly suggests that a modest increase of charge inside the substrate binding chamber facilitates the insertion of σ^M-regulated proteins overproduced under YhdL depletion conditions, whereas a further increase may be detrimental to the activity or the stability of the insertase.

Each of these 17 SpoIIIJ variants can alleviate the stress imposed by high σ^M activity and support growth of the YhdL depletion strain (Fig. S3C), and increase the colony size of the *yhdK* mutant by up to 74% (Fig. 3C). We also found 16 of these 17 variants can support growth of a YidC2 depletion strain (Fig. S3D). Only the SpoIIIJ R72 K140 R144 variant was unable to support cell growth under these conditions, suggesting that it is compromised in the ability to insert proteins essential for cell growth, despite its ability to modestly increase colony size of the *yhdK* mutant (31%).

SpoIIIJ also inserts MifM into the membrane, which serves as a sensor of SpoIIIJ function to regulate expression of *yidC2* [21, 26]. We used a *yidC2'-lacZ* translational fusion reporter to measure the ability of each SpoIIIJ variant to insert MifM. A WT 168 strain exhibited very low level of *yidC2'-lacZ* activity in the presence of native *spoIIIJ* expression (~42 Miller Units (MU), Fig. 3D), and deletion of *spoIIIJ* increased the reporter activity by about 3-fold (~132 MU, Fig. 3D). Complementation of a *spoIIIJ* null mutant with the 168 version of *spoIIIJ* (single positive charge at R73) at the *thrC* locus reduced the reporter activity to ~101 MU (Fig. 3D). The lack of complete complementation may be caused by the location of the gene, as the native locus is close to the origin of the chromosome and thus has higher copy number than *thrC* in fast growing cells. Indeed, under our growth condition (late exponential phase in LB at 37°C), less SpoIIIJ protein was detected in the *thrC*::*spoIIIJ* complementation strain than the WT (Fig. 3D).

Using this strain background, we found that most of the SpoIIIJ variants with double positive charge appear to have higher MifM insertion ability as they exhibited lower *yidC2'-lacZ* activity than the WT protein. Interestingly, the three mutants with double positive charge that have the largest colony size in a *yhdK* mutant background (R73 K140, K140 R144, and K140 R228), also showed the lowest *yidC2'-lacZ* activity, consistent with the hypothesis that they have higher insertase activity for both MifM and for proteins that contribute to toxicity in strains with high σ^M-activity. Conversely, one mutant with a nominal triple positive charge (R76 K140 R228) exhibited a strong increase in colony size in the *yhdK* mutant background (Fig. 3C), but appeared to have low MifM insertion activity (high *yidC2'-lacZ* expression; Fig. 3D). Overall these results suggest that increasing the positive charge inside the substrate binding groove affects the efficiency of inserting membrane proteins, with several variants that appear to enhance the insertion efficiency

293 for both MifM and σ^M-regulated proteins, while also retaining the ability to insert essential
294 membrane proteins.
295
296 **High σ^M activity causes a cascade of stresses that can be partially compensated by its regulon**
297 SpoIIIJ functions as a membrane insertase, by either independently inserting some single
298 pass membrane proteins or by functioning as part of the Sec translocon to facilitate the folding of
299 the translocated proteins [18, 27]. The finding that SpoIIIJ^{Q140K} can suppress growth defects caused
300 by high σ^M leads us to reason that the toxicity of high σ^M is caused by overexpression of membrane
301 proteins that overwhelm the secretion system, and that SpoIIIJ^{Q140K} suppresses this stress by
302 functioning as a more efficient insertase/foldase or chaperon. In *B. subtilis*, membrane secretion
303 stress is sensed by the CssRS (control of secretion stress regulator/sensor) two component system.
304 In the presence of membrane secretion stress, caused either by overproduction of secreted proteins
305 or high temperature, CssR upregulates expression of membrane proteases HtrA (high temperature
306 requirement A) and HtrB to facilitate the re-folding or degradation of misfolded proteins [28, 29].
307 To test whether high σ^M causes secretion stress, we constructed a P_{htrA}-*lux* reporter to
308 monitor induction of the CssR-regulon. Indeed, P_{htrA} activity was increased about ten-fold in a
309 *yhdK* mutant, and this induction can be reduced by the SpoIIIJ^{Q140K} allele by about 70% (Fig. 4A).
310 To evaluate the role of the CssRS system in alleviating the membrane protein overproduction stress
311 under high σ^M condition, we constructed mutants missing components of the CssR regulon and
312 used *yhdK* mutant colony size as a measure of fitness. Surprisingly, we found that neither CssR-
313 regulated membrane protease (HtrA and HtrB) is important for fitness of the *yhdK* mutant as
314 judged by the effect of their deletion on colony size. Deletion of the response regulator CssR
315 abolished the induction of the regulon [29], and has no effect on the fitness of *yhdK* mutant. In

316 contrast to a previous report [29], the absence of CssS increased transcription of P_{htrA}-*lux* reporter
317 by ~80-fold. This suggests that CssS may act both as a sensor kinase to activate CssR and the
318 regulon under induction conditions, and also as a phosphatase to deactivate CssR in the absence
319 of induction signals, as also noted for sensor kinases in other two component systems [30].

320 Deletion of *cssS* reduced *yhdK* mutant colony size by over 60% (Fig. 4B), and the reduction
321 of colony size is reversed in a *cssS htrB* double mutant, suggesting that high HtrB activity is
322 detrimental for the *yhdK* mutant. Consistently, when *htrB* but not *htrA* was overexpressed using
323 the $P_{spac(hy)}$ promoter, the colony size of *yhdK* mutant was reduced by about 50% (Fig. 4B). Deletion
324 of these genes in the WT 168 background did not have much effect on the colony size (Fig. S4A).
325 These results suggest that the *yhdK* mutant is sensitive to the overproduction of membrane
326 proteases. Single deletion of other proteases, including SipT, SipS, HtpX, PrsW and GlpG in a
327 *yhdK* null mutant was also not detrimental, and in some cases led to a small beneficial effect in
328 colony size (Fig S4B), again indicating that membrane protease activity is not beneficial for the
329 *yhdK* mutant. We speculate that under high σ^M conditions, the overproduced proteins may cause a
330 backlog of membrane proteins that require a longer time to correctly insert and fold in the
331 membrane. Some of these proteins may be essential for cell growth and are vulnerable to
332 degradation by membrane proteases.

333 Misfolding of membrane proteins, as well as jamming the Sec translocon by hybrid
334 proteins, leads to the generation of reactive oxygen species (ROS) and ultimately DNA damage
335 [31, 32]. To test whether high σ^M also triggers a similar cascade of stresses, we performed
336 quantitative RT-PCR to measure induction of representative stress genes. Indeed, the high σ^M
337 activity in the *yhdK* null mutant was correlated with strong induction of genes involved in secretion
338 stress (*secG*, *cssR*), oxidative stress (*katA*, *sodA*), and DNA repair (*lexA*, *dinB* and *recA*) (Fig 4C).

The induction of these stress response genes was largely suppressed in the presence of the s*poIIIJ*^{Q140K} allele, suggesting that their induction is a downstream effect resulting from inefficient insertion of membrane proteins (Fig 4C).

Interestingly, while many genes in the σ^M regulon are involved in the synthesis and maintenance of the cell wall, there are also genes involved in regulation of redox balance (*spx* and the Spx regulon), DNA repair and recombination (for example, *radA*, *radC* and *recU*), and ppGpp synthesis and stringent response (*sasA*) [3]. There is also a candidate σ^M promoter associated with the *secDF* operon [3]. This suggests that a subset of genes in the σ^M regulon are involved in compensating for stresses associated with upregulation of σ^M. Indeed, deletion of *secDF*, *sasA* or the P_M of *spx* dramatically reduced the colony size of the *yhdK* mutant (Fig. 4D), while there was very little effect noted in the WT background (Fig. S4C). Thus, these genes seem to play an important role in cell fitness specifically under conditions of high σ^M expression. Deleting single genes inside the Spx regulon in the *yhdK* mutant did not lead to noticeable reduction of colony size (Fig. S4D), suggesting functional redundancy within the Spx regulon.

Among the 69 genes currently assigned to the σ^M regulon according to SubtiWiki [33], 38 code for membrane-associated or secreted proteins (Table S4). To demonstrate the burden these membrane proteins may cause when overexpressed under high σ^M condition, we mutated the σ^M-dependent promoters (P_M) for genes important for the elongasome and the divisome and tested the consequence on fitness measured by colony size of the *yhdK* mutant. We focused on a P_M inside *maf* gene that transcribes *radC-mreB-mreC-mreD-minC-minD* operon, a P_M upstream of *rodA* gene, and a P_M inside *murG* that contributes to transcription of the *murB-divIB-ylxW-ylxX-sbp-ftsA-ftsZ* operon (Fig 4E). Mutation of these three promoters individually or in combination had little effect on the colony size of the WT strain (Fig. S4E), since these genes are also expressed

362 from σ^A-dependent promoters. In a *yhdK* mutant, however, mutation of P_M(*maf*) and P_M(*murG*) led
363 to an additive increase of colony size, while mutation of P_M(*rodA*) led to a small detrimental effect
364 (Fig. 4F). We conclude that overexpression of genes downstream of P_M(*maf*) and P_M(*murG*) may
365 overwhelm the membrane-protein insertion pathway, and thereby contribute to a net negative
366 effect on cell fitness. Consistent with this idea, in cells expressing SpoIIIJ^{Q140K}, the beneficial effect
367 of mutating P_M(*maf*) and P_M(*murG*) was largely abolished (Fig. 4G).
368

369 ## Discussion

370 The YidC membrane protein insertase is the bacterial representative of the
371 YidC/Oxa1/Alb3 protein family of evolutionary conserved integral membrane proteins [18, 27].
372 In *E. coli*, YidC is required for the assembly of one or more essential protein complexes that reside
373 in the inner membrane, including subunits of the energy generating F_1F_O ATPase and NADH
374 dehydrogenase I [34]. Although YidC can function in concert with the SecYEG translocon as a
375 foldase/chaperone, YidC can also function independently for the insertion of small membrane
376 proteins with one or two transmembrane segments [35].

377 *Bacillus subtilis* encodes two YidC paralogs, SpoIIIJ and YidC2 (formerly YqjG). Either
378 protein can support growth of *B. subtilis*, but a double mutant is inviable. Under most conditions
379 SpoIIIJ is the functional YidC homolog and is responsible for insertion of transmembrane proteins,
380 including the F_1F_O ATPase [19]. MifM, a membrane protein encoded upstream of *yidC2*, is also a
381 substrate of SpoIIIJ and serves as a sensor for SpoIIIJ activity [21]. In the absence of SpoIIIJ
382 activity, the translational pause caused by the membrane insertion of MifM is abolished and YidC2
383 is translationally activated [26, 36]. Although either SpoIIIJ or YidC2 can support growth, they
384 appear to differ in the efficacy of inserting specific proteins: cells lacking SpoIIIJ are impaired in

sporulation [20], whereas those lacking YidC2 have decreased competence [23]. The relationship between YidC protein sequence and the selection of specific client proteins is poorly understood. In cells depleted for both SpoIIIJ and YidC2 there was a substantial upregulation in expression of the Clp protease system and the LiaIH membrane-stress proteins that are regulated by the LiaRS two-component system [23]. This suggests that impairment of membrane protein insertion leads to an accumulation of misfolded proteins and disruption of the cell membrane.

One critical feature required for YidC function, as first visualized in the structure of the *B. halodurans* YidC protein [16], is a hydrophilic substrate-binding channel postulated to interact transiently with transmembrane segments of nascent integral membrane proteins. In YidC proteins the first transmembrane region (TM1) contains a conserved Arg residue that is essential for function in many, but not all, YidC orthologs [37]. This positively charged residue is postulated to form a salt-bridge with single-pass transmembrane client proteins with acidic residues in their amino-terminal region [16]. Remarkably, the function of this conserved Arg residues (R73 in *Bacillus* SpoIIIJ) can be replaced by Arg residues introduced at any of six other positions in transmembrane segments of YidC [25].

In this work, we have described an unusual variant of SpoIIIJ found in *B. subtilis* strain PY79 which contains the conserved R73 residue and additionally a second positively charged residue (K140) at a position that can functionally replace R73. This variant SpoIIIJ protein ($SpoIIIJ^{Q140K}$) is necessary and sufficient for *B. subtilis* to survive high level expression of the σ^M regulon. By screening of a library of SpoIIIJ variants with different charges, we revealed that all SpoIIIJ proteins that enable cells to tolerate loss of *yhdL* contain at least two, and in some cases three, positively charged residues in this channel. We postulated that these SpoIIIJ variants may be more capable of accommodating the increased expression of membrane proteins under σ^M

control. Support for this hypothesis derives from experiments in which the deletion of individual σ^M-dependent promoters that control operons encoding multiple integral membrane proteins was found to improve fitness of strains with high σ^M activity. Thus we reason that the relevant feature of SpoIIIJ^{Q140K} is the presence of increased positive charge in the substrate-binding channel, which probably results in an increased insertase/foldase activity for specific σ^M-regulated membrane proteins.

Our results have clarified the nature of the lethality associated with a *yhdL* deletion that unleashes high level σ^M activity. In strains with elevated σ^M activity there is an increased flux of proteins targeted to the inner membrane and a subset of these may be inefficiently inserted by the native SpoIIIJ protein. This can result in a jamming of YidC-dependent protein translocation and a disruption of membrane function. The downstream sequelae associated with this disruption includes misfolding of proteins and induction of the secretion stress response (CssR), as well as genes associated with oxidative stress and DNA damage. These types of stresses may explain, in part, the inclusion of appropriate compensatory functions (including Spx, some DNA repair functions, and SecDF) as part of the σ^M regulon. It is presently unclear why the *spoIIIJ*^{Q140K} allele arose in the PY79 strain, or what conditions may have led to its selection. However, this strain was derived from strains treated with chemical mutagens to cure the endogenous prophage SPß [14] and this or other selection conditions may have contributed to emergence of this mutation. Further studies will be required to better understand how variations in YidC structure can fine-tune the substrate selectivity of this essential membrane protein insertase, and the stresses that arise when this system is challenged by the induction of highly expressed membrane proteins.

Material and Methods

Strains, plasmids and growth condition

All strains used in this work are listed in Table S5, and all DNA primers are listed in Table S6. Bacteria were routinely grown in liquid lysogeny broth (LB) with vigorous shaking, or on plates (1.5% agar; Difco) at 37 ˚C unless otherwise stated. LB medium contains 10 g tryptone, 5 g yeast extract, and 5 g NaCl per liter. Plasmids were constructed using standard methods [38], and amplified in *E. coli* DH5α or TG1 before transforming into *B. subtilis*. For selection of transformants, 100 μg ml^{-1} ampicillin or 30 μg ml^{-1} kanamycin was used for *E. coli*. Antibiotics used for selection of *B. subtilis* transformants include: kanamycin 15 μg ml^{-1}, spectinomycin 100 μg ml^{-1}, macrolide-lincosamide-streptogramin B (MLS, contains 1 μg ml^{-1} erythromycin and 25 μg ml^{-1} lincomycin), and chloramphenicol 10 μg ml^{-1}. For spot dilution assays, cells were first grown in liquid culture at 37 ˚C with shaking to mid-exponential phase (OD_{600} ~0.3-0.4), washed twice in LB medium without inducer, then serial diluted in LB medium without inducer. 10 μl of each diluted culture was then spotted onto plates and allowed to dry before incubation at 37 ˚C for 12-24 hours.

Genetic techniques

Chromosomal and plasmid DNA transformation was performed as previously stated [39]. The pPL82 plasmid-based $P_{spac(hy)}$ overexpression constructs were sequencing confirmed before linearized and integrated into the *amyE* locus [24]. The pAX01 plasmid-based P_{xylA} overexpression constructs were sequencing confirmed before linearized and integrated into the *ganA* locus [40]. The *ganA*::P_{xylA}-*yhdL-cat* and *thrC*::P_M-*spoVG-lacZ-spec* constructs were made with LFH PCR to avoid antibiotic marker conflicts [10]. Markerless in-frame deletion mutants were constructed from BKE or BKK strains as described [41]. Briefly, BKE or BKK strains were acquired from the

454 *Bacillus* Genetics Stock Center (http://www.bgsc.org), chromosomal DNA was extracted, and the
455 mutation containing an *erm*^{R} (for BKE strains) or *kan*^{R} (for BKK strains) cassette was transformed
456 into our WT 168 strain. The antibiotic cassette was subsequently removed by introduction of the
457 Cre recombinase carried on plasmid pDR244, which was later cured by growing at the non-
458 permissive temperature of 42 ˚C. Gene deletions were confirmed by PCR screening using flanking
459 primers. Unless otherwise described, all PCR products were generated using *B. subtilis* 168 strain
460 chromosomal DNA as template. DNA fragments used for gene over-expression were verified by
461 sequencing. Null mutant constructions were verified by PCR.

462 Mutations to selectively inactivate σ^{M}-dependent promoters were generated by either
463 promoter deletion (*rodA*) or by inactivating point mutations (*murG*, *maf*, *spx*). To inactivate
464 P_M(*rodA*), a 91 bp region containing the P_M (located upstream of a σ^{A}-dependent promoter) was
465 deleted using CRISPR. The resulting deletion had a junction sequence of:
466 CACATTATCGC/TTTCGTGTAGC. The point mutations inactivating *murG* and *maf* both
467 changed the -10 region sequence from consensus, CGTC, to TGTT. The P_M* mutation inactivating
468 the promoter regulating the *yjbC-spx* operon is a 3 bp substitution changing the -10 region from
469 consensus, CGTC, to AAGT, as previously described [42].

470 Mutations of *spoIIIJ* at native locus, as well as ΔP_M-*rodA* were constructed using a
471 clustered regularly interspaced short palindromic repeats (CRISPR)-based mutagenesis method as
472 previously described [10]. Briefly, possible protospacer adjacent motifs (PAM) site, which is NGG
473 for *Streptococcus pyogenes* Cas9, was identified and off-target sites were checked against *B.*
474 *subtilis* genome using BLAST. If no off-target site was identified, the PAM site was chosen and
475 20 bps upstream of the site were used as sgRNA and cloned into vector pJOE8999 [43]. The repair
476 template was generated by joining two or more PCR products, with intended mutation (with

477 additional mutation to abolish gRNA recognition if necessary) introduced by PCR primers, and
478 cloned into the pJOE8999-sgRNA vector. DNA sequence for amino acid substitution was chosen
479 according to the preferred codons of *B. subtilis* [44]. The pJOE8999 derivative containing both the
480 sgRNA and repair template was then cloned into competent cells of *E. coli* strain TG1 to produce
481 concatemer plasmids, which were transformed into *B. subtilis* at 30°C. Transformants were then
482 grown at 42°C to cure the plasmid, and intended mutations were confirmed by sequencing. ΔP_M-
483 *rodA* was constructed with repair template amplified using primers 7426, 7427, 7428 and 7429,
484 and the gRNA constructed using 7430 and 7431. SpoIIIJ^{Q140K} mutation in 168 was constructed with
485 repair template amplified using primers 7868, 7869, 7870 and 7871, and the gRNA constructed
486 using 7866 and 7867. SpoIIIJ^{K140Q} mutation in PY79 was constructed with repair template
487 amplified using primers 7866, 8247, 8246 and 7871, and the gRNA constructed using 8248 and
488 8249. SpoIIIJ^{R73A} mutation was constructed with repair template amplified using strain 168
489 genomic DNA as template with primers 7868, 8280, 8281 and 7871, and the gRNA constructed
490 using 8278 and 8279. SpoIIIJ^{R73AQ140K} mutation was constructed with the same primer sets for
491 SpoIIIJ^{R73A} mutation, expect the repair template was amplified using strain PY79 genomic DNA.
492 All constructs were sequencing confirmed.

493 SpoIIIJ library of different positive charges were constructed using degenerate primers and
494 LFH PCR. Four DNA fragments were amplified and joined using LFH PCR. The fragments
495 include one with part of gene *hom* and *thrC* (amplified with primers 8766 and 8767), one with the
496 spoIIIJ gene from 168 (amplified with primers 8768 and 8681, containing the native promoter and
497 ribosomal binding site), one with a spec^R cassette (amplified with primers 8682 and 8769), and
498 one with part of *thrC* and full length of *thrB* (amplified with primers 8770 and 8771). The joined
499 PCR product was first transformed into strain 168 to generate HB23976. Then using genomic

DNA of HB23976 as template, four new DNA fragments were amplified using degenerate primer pairs 8766 and 8689, 8686 and 8690, 8687 and 8691, and 8688 and 8771. These fragments were joined together using LFH PCR and the joined PCR product (more than 10 μg DNA) was expected to contain all 128 possible combinations of SpoIIIJ charge from 0 to +7. The PCR product library was used to transform strain 168, and more than ten-thousand transformants (from 20 plates, each contains more than 500 colonies) were pooled together to extract genomic DNA to form a virtually equivalent DNA library of the *spoIIIJ* variants. This genomic DNA library provides high transformation efficiency and was used to transform a *yhdL* depletion strain (HB23953) and transformants were selected on LB plate supplemented with X-gal but no xylose for *yhdL* induction. More than 200 transformants were re-streaked onto fresh LB plate with X-gal but no xylose to confirm robust growth under high SigM condition, and 103 of them were Sanger sequenced for the *thrC-spoIIIJ-spec* region to identify the *spoIIIJ* variants.

Whole genome re-sequencing and sequence analysis

Chromosomal DNA of suppressor strains was extracted using Qiagen DNeasy Blood & Tissue Kit. DNA was then sent to Cornell University Institute of Biotechnology for sequencing using Illumina HiSeq2500 with Single-end 100 bp reads. Sequencing results were analyzed using CLC workbench version 8.5.1 and mapped to the genome of strain 168 (reference accession number NC_000964.3). Note that our working stock of *B. subtilis* 168 has 21 SNPs compared to the cited reference sequence, and these common SNPs were not considered, and only newly introduced SNPs from the PY79 strain were tabulated (Table S2). Unmapped reads were de novo assembled and contigs larger than 1 kb were BLASTed against genome of strain PY79 (reference accession number NC_022898.1). Single nucleotide variants (SNVs) were detected using default

523 settings, and gene deletions larger than 300 bps were identified by manually scanning regions of
524 low coverage.
525
526 **Colony size measurement**
527 Colony size was measured using Fiji Image J [45]. Briefly, bacterial cells were grown in liquid LB
528 medium at 37°C with vigorous shaking to mid-exponential phase (OD_{600}~0.3-0.4), then serial
529 diluted to desired concentrations. Diluted cells were plated onto fresh LB plates (15 ml medium
530 per plate, the diameter of the plate is 10 cm and the height 15 mm, VWR, US, Catalog number
531 25384-342), and multiple dilutions were used. Plates were incubated at 37 °C for 24 hours. Plates
532 containing less than 100 separate single colonies were used for size measurement, because this
533 number of colonies per plate ensures sufficient sample size and does not cause reduced colony size
534 due to crowdedness and nutrient limitation. Pictures of plates were taken with a ruler as a length
535 reference, and colony size was measured using Fiji Image J per software's instruction. For each
536 strain, at least 100 colonies were measured, and box and whisker plots were used.
537
538 **Luciferase reporter construction and measurement**
539 Luciferase reporter construction and measurement was performed as previous described
540 [46]. The luciferase reporters were constructed by inserting the tested promoters into the
541 multicloning sites of pBS3C*lux* [47]. The promoter P_{htrA} was amplified using primers 8403 and
542 8404. For luciferase measurements, 1 µl of exponentially growing cells were inoculated into 99 µl
543 of fresh medium in a 96 well plate, incubated at 37 °C with shaking using a SpectraMax i3x plate
544 reader, and OD_{600} and luminescence were measured every 12 min. The data was analyzed using

SoftMax Pro 7.0 software. Promoter activity was normalized by dividing the relative light units (RLU) by OD_{600}.

Phase contrast microscopy

Cells were grown in liquid LB medium to exponential phase (OD_{600} ~0.4) and loaded on saline (0.90% NaCl, w/v) agarose pads (0.8% final concentration) on a glass slide. Phase contrast images were taken using a Leica DMi8 microscope equipped with a 100x immersion objective and Leica Application Suite X software.

Western blot

Western blot was performed as described previously [42]. Briefly, cells were grown in 5 ml LB medium in a 20 ml test tube a 37 °C with vigorous shaking. Inducer IPTG or xylose were added when required by the construct to induce SpoIIIJ. After reaching exponential phase (OD_{600}~0.3-0.4), 1 ml cells were pelleted by centrifugation at 4°C, resuspended in 100 µl pre-chilled buffer (containing 25 µl 4X Laemmli Sample buffer (Bio-Rad, USA), 10 µl 1M DTT, 65 µl H_2O) and kept on ice. Cells were then lysed and crude cell lysate was loaded to a 4-20% SDS-PAGE stain-free gel for electrophoresis. The gel was visualized using ImageLab with stain-free gel protocol. Proteins were then transferred onto a PVDF membrane using the TransBlot Turbo Transfer System (Bio-Rad, USA), and immune blotting was performed using anti-SpoIIIJ antiserum. The blot was visualized using the Clarity Western ECL substrate (Bio-Rad) and ImageLab software. Band intensity was calculated using the ImageLab software and normalized using total protein amount according to SDS-PAGE gel image.

568 **β-galactosidase assay for *yidC2'-lacZ***

569 Bacterial cells containing the *yidC2'-lacZ* translational fusion were grown to late exponential
570 phase (OD_{600} 0.6-0.8) in 96-well plates with 200 µl LB medium per well at 37 °C with vigorous
571 shaking. Cells were pelleted by centrifugation, resuspended in Z buffer supplemented with DTT
572 (Dithiothreitol, 400 nM final concentration), and lysed by lysozyme. OD_{600} was measured before
573 lysozyme treatment. After lysis, ONPG (ortho-nitrophenyl-β-galactoside) was added and OD_{420}
574 and OD_{550} were measured every 2 minutes. Product accumulation was calculated using formula
575 $product=1000\times[OD_{420}-(1.75\times OD_{550})]$ and plotted against time. The slope of the linear part of the
576 product accumulation curve was calculated using Excel and Miller Unit (MU) was calculated using
577 formula $MU=Slope/OD_{600}/V$, where V is the volume of cells used for the reaction (200 µl).
578
579 **RNA extraction and qRT-PCR**
580 Cells were grown to mid-exponential phase (OD_{600} ~0.4) and RNA was extracted using RNeasy
581 Mini Kit (Qiagen). The extracted was then treated with DNase I (Invitrogen) and the quality of
582 RNA was checked with electrophoresis. RNA was then reverse transcribed into cDNA using High-
583 Capacity cDNA Reverse Transcription Kit (Applied Biosystems). Quantitative real-time PCR
584 (qRT-PCR) was performed using SYBR Green (BioRad) and the *topA* gene was used for reference
585 of data normalization.
586

587 **Acknowledgements**: We thank Dr. Shinobu Chiba for providing the *yidC2'-lacZ* translational
588 fusion reporter and antiserum for SpoIIIJ, Dr. David Rudner and Alexander Meeske for strain
589 BAM1077, Dr. Vaidehi Patel and Wen-Wen Zhou for providing the P_M* mutations for the *murG*
590 and *maf* operons, and Dr. Tobias Doerr for valuable discussions and sharing equipment. We also

591 thank Dr. Pete Chandrangsu and Ahmed Gaballa for help with experimental design and
592 interpretation, and Daniel Roistacher for helping with experiments.

593

594 Author Contributions
595 Conceptualization: Heng Zhao, John D. Helmann
596 Funding acquisition: John D. Helmann.
597 Investigation: Heng Zhao, Anita Sachla
598 Project administration: John D. Helmann.
599 Writing - original draft: Heng Zhao, John D. Helmann.
600 Writing - review & editing: Heng Zhao, Anita Sachla, John D. Helmann.

601

602

603 **References**

604

605 1. Helmann JD. *Bacillus subtilis* extracytoplasmic function (ECF) sigma factors and defense
606 of the cell envelope. Curr Opin Microbiol. 2016;30:122-32. Epub 2016/02/24. doi:
607 10.1016/j.mib.2016.02.002. PubMed PMID: 26901131; PubMed Central PMCID:
608 PMCPMC4821709.
609 2. Sineva E, Savkina M, Ades SE. Themes and variations in gene regulation by
610 extracytoplasmic function (ECF) sigma factors. Curr Opin Microbiol. 2017;36:128-37. doi:
611 10.1016/j.mib.2017.05.004. PubMed PMID: 28575802; PubMed Central PMCID:
612 PMCPMC5534382.
613 3. Eiamphungporn W, Helmann JD. The *Bacillus subtilis* sigma(M) regulon and its
614 contribution to cell envelope stress responses. Mol Microbiol. 2008;67(4):830-48. Epub
615 2008/01/09. doi: 10.1111/j.1365-2958.2007.06090.x. PubMed PMID: 18179421; PubMed
616 Central PMCID: PMCPMC3025603.
617 4. Horsburgh MJ, Moir A. Sigma M, an ECF RNA polymerase sigma factor of *Bacillus*
618 *subtilis* 168, is essential for growth and survival in high concentrations of salt. Mol
619 Microbiol. 1999;32(1):41-50. Epub 1999/04/27. PubMed PMID: 10216858.
620 5. Luo Y, Helmann JD. Analysis of the role of *Bacillus subtilis* sigma(M) in beta-lactam
621 resistance reveals an essential role for c-di-AMP in peptidoglycan homeostasis. Mol
622 Microbiol. 2012;83(3):623-39. Epub 2012/01/04. doi: 10.1111/j.1365-2958.2011.07953.x.
623 PubMed PMID: 22211522; PubMed Central PMCID: PMCPMC3306796.
624 6. Meeske AJ, Riley EP, Robins WP, Uehara T, Mekalanos JJ, Kahne D, et al. SEDS proteins
625 are a widespread family of bacterial cell wall polymerases. Nature. 2016;537(7622):634-8.
626 Epub 2016/08/16. doi: 10.1038/nature19331. PubMed PMID: 27525505; PubMed Central
627 PMCID: PMCPMC5161649.
628 7. Asai K. Anti-sigma factor-mediated cell surface stress responses in *Bacillus subtilis*. Genes
629 Genet Syst. 2018;92(5):223-34. Epub 2018/01/19. doi: 10.1266/ggs.17-00046. PubMed
630 PMID: 29343670.
631 8. Woods EC, McBride SM. Regulation of antimicrobial resistance by extracytoplasmic
632 function (ECF) sigma factors. Microbes Infect. 2017;19(4-5):238-48. doi:

633 10.1016/j.micinf.2017.01.007. PubMed PMID: 28153747; PubMed Central PMCID:
634 PMCPMC5403605.
635 9. Yoshimura M, Asai K, Sadaie Y, Yoshikawa H. Interaction of *Bacillus subtilis*
636 extracytoplasmic function (ECF) sigma factors with the N-terminal regions of their
637 potential anti-sigma factors. Microbiology. 2004;150(Pt 3):591-9. doi:
638 10.1099/mic.0.26712-0. PubMed PMID: 14993308.
639 10. Zhao H, Roistacher DM, Helmann JD. Deciphering the essentiality and function of the
640 anti-sigma(M) factors in *Bacillus subtilis*. Mol Microbiol. 2019. doi: 10.1111/mmi.14216.
641 PubMed PMID: 30715747.
642 11. Murakami T, Haga K, Takeuchi M, Sato T. Analysis of the *Bacillus subtilis spoIIIJ* gene
643 and its Paralogue gene, *yqjG*. J Bacteriol. 2002;184(7):1998-2004. doi:
644 10.1128/jb.184.7.1998-2004.2002. PubMed PMID: 11889108; PubMed Central PMCID:
645 PMCPMC134917.
646 12. Tjalsma H, Bron S, van Dijl JM. Complementary impact of paralogous Oxa1-like proteins
647 of *Bacillus subtilis* on post-translocational stages in protein secretion. J Biol Chem.
648 2003;278(18):15622-32. doi: 10.1074/jbc.M301205200. PubMed PMID: 12586834.
649 13. Zeigler DR, Pragai Z, Rodriguez S, Chevreux B, Muffler A, Albert T, et al. The origins of
650 168, W23, and other *Bacillus subtilis* legacy strains. J Bacteriol. 2008;190(21):6983-95.
651 Epub 2008/08/30. doi: 10.1128/JB.00722-08. PubMed PMID: 18723616; PubMed Central
652 PMCID: PMCPMC2580678.
653 14. Schroeder JW, Simmons LA. Complete Genome Sequence of *Bacillus subtilis* Strain
654 PY79. Genome Announc. 2013;1(6). Epub 2013/12/21. doi: 10.1128/genomeA.01085-13.
655 PubMed PMID: 24356846; PubMed Central PMCID: PMCPMC3868870.
656 15. Dubnau D, Cirigliano C. Fate of transforming DNA following uptake by competent
657 *Bacillus subtilis*. Formation and properties of products isolated from transformed cells
658 which are derived entirely from donor DNA. J Mol Biol. 1972;64(1):9-29. Epub
659 1972/02/28. PubMed PMID: 4622632.
660 16. Kumazaki K, Chiba S, Takemoto M, Furukawa A, Nishiyama K, Sugano Y, et al.
661 Structural basis of Sec-independent membrane protein insertion by YidC. Nature.
662 2014;509(7501):516-20. Epub 2014/04/18. doi: 10.1038/nature13167. PubMed PMID:
663 24739968.

17. Tsirigotaki A, De Geyter J, Sostaric N, Economou A, Karamanou S. Protein export through the bacterial Sec pathway. Nat Rev Microbiol. 2017;15(1):21-36. Epub 2016/11/29. doi: 10.1038/nrmicro.2016.161. PubMed PMID: 27890920.

18. Hennon SW, Soman R, Zhu L, Dalbey RE. YidC/Alb3/Oxa1 Family of Insertases. J Biol Chem. 2015;290(24):14866-74. Epub 2015/05/08. doi: 10.1074/jbc.R115.638171. PubMed PMID: 25947384; PubMed Central PMCID: PMCPMC4463434.

19. Saller MJ, Fusetti F, Driessen AJ. *Bacillus subtilis* SpoIIIJ and YqjG function in membrane protein biogenesis. J Bacteriol. 2009;191(21):6749-57. Epub 2009/09/01. doi: 10.1128/JB.00853-09. PubMed PMID: 19717609; PubMed Central PMCID: PMCPMC2795313.

20. Errington J, Appleby L, Daniel RA, Goodfellow H, Partridge SR, Yudkin MD. Structure and function of the *spoIIIJ* gene of *Bacillus subtilis*: a vegetatively expressed gene that is essential for sigma G activity at an intermediate stage of sporulation. J Gen Microbiol. 1992;138(12):2609-18. Epub 1992/12/01. doi: 10.1099/00221287-138-12-2609. PubMed PMID: 1487728.

21. Chiba S, Ito K. MifM monitors total YidC activities of *Bacillus subtilis*, including that of YidC2, the target of regulation. J Bacteriol. 2015;197(1):99-107. Epub 2014/10/15. doi: 10.1128/JB.02074-14. PubMed PMID: 25313395; PubMed Central PMCID: PMCPMC4288694.

22. Corte L, Valente F, Serrano M, Gomes CM, Moran CP, Jr., Henriques AO. A conserved cysteine residue of *Bacillus subtilis* SpoIIIJ is important for endospore development. PLoS One. 2014;9(8):e99811. Epub 2014/08/19. doi: 10.1371/journal.pone.0099811. PubMed PMID: 25133632; PubMed Central PMCID: PMCPMC4136701.

23. Saller MJ, Otto A, Berrelkamp-Lahpor GA, Becher D, Hecker M, Driessen AJ. *Bacillus subtilis* YqjG is required for genetic competence development. Proteomics. 2011;11(2):270-82. Epub 2011/01/05. doi: 10.1002/pmic.201000435. PubMed PMID: 21204254.

24. Quisel JD, Burkholder WF, Grossman AD. In vivo effects of sporulation kinases on mutant Spo0A proteins in *Bacillus subtilis*. J Bacteriol. 2001;183(22):6573-8. doi: 10.1128/JB.183.22.6573-6578.2001. PubMed PMID: 11673427; PubMed Central PMCID: PMCPMC95488.

25. Shimokawa-Chiba N, Kumazaki K, Tsukazaki T, Nureki O, Ito K, Chiba S. Hydrophilic microenvironment required for the channel-independent insertase function of YidC protein. Proc Natl Acad Sci U S A. 2015;112(16):5063-8. Epub 2015/04/10. doi: 10.1073/pnas.1423817112. PubMed PMID: 25855636; PubMed Central PMCID: PMCPMC4413333.

26. Chiba S, Ito K. Multisite ribosomal stalling: a unique mode of regulatory nascent chain action revealed for MifM. Mol Cell. 2012;47(6):863-72. Epub 2012/08/07. doi: 10.1016/j.molcel.2012.06.034. PubMed PMID: 22864117.

27. Kuhn A, Kiefer D. Membrane protein insertase YidC in bacteria and archaea. Mol Microbiol. 2017;103(4):590-4. Epub 2016/11/24. doi: 10.1111/mmi.13586. PubMed PMID: 27879020.

28. Hyyrylainen HL, Bolhuis A, Darmon E, Muukkonen L, Koski P, Vitikainen M, et al. A novel two-component regulatory system in *Bacillus subtilis* for the survival of severe secretion stress. Mol Microbiol. 2001;41(5):1159-72. PubMed PMID: 11555295.

29. Darmon E, Noone D, Masson A, Bron S, Kuipers OP, Devine KM, et al. A novel class of heat and secretion stress-responsive genes is controlled by the autoregulated CssRS two-component system of *Bacillus subtilis*. J Bacteriol. 2002;184(20):5661-71. doi: 10.1128/jb.184.20.5661-5671.2002. PubMed PMID: 12270824; PubMed Central PMCID: PMCPMC139597.

30. Podgornaia AI, Laub MT. Determinants of specificity in two-component signal transduction. Curr Opin Microbiol. 2013;16(2):156-62. Epub 2013/01/29. doi: 10.1016/j.mib.2013.01.004. PubMed PMID: 23352354.

31. Takahashi N, Gruber CC, Yang JH, Liu X, Braff D, Yashaswini CN, et al. Lethality of MalE-LacZ hybrid protein shares mechanistic attributes with oxidative component of antibiotic lethality. Proc Natl Acad Sci U S A. 2017. Epub 2017/08/11. doi: 10.1073/pnas.1707466114. PubMed PMID: 28794281; PubMed Central PMCID: PMCPMC5576823.

32. Kohanski MA, Dwyer DJ, Wierzbowski J, Cottarel G, Collins JJ. Mistranslation of membrane proteins and two-component system activation trigger antibiotic-mediated cell death. Cell. 2008;135(4):679-90. Epub 2008/11/18. doi: 10.1016/j.cell.2008.09.038. PubMed PMID: 19013277; PubMed Central PMCID: PMCPMC2684502.

33. Zhu B, Stulke J. SubtiWiki in 2018: from genes and proteins to functional network annotation of the model organism *Bacillus subtilis*. Nucleic Acids Res. 2018;46(D1):D743-D8. Epub 2018/05/23. doi: 10.1093/nar/gkx908. PubMed PMID: 29788229; PubMed Central PMCID: PMCPMC5753275.

34. Price CE, Driessen AJ. YidC is involved in the biogenesis of anaerobic respiratory complexes in the inner membrane of *Escherichia coli*. J Biol Chem. 2008;283(40):26921-7. doi: 10.1074/jbc.M804490200. PubMed PMID: 18635537.

35. Dalbey RE, Kuhn A, Zhu L, Kiefer D. The membrane insertase YidC. Biochim Biophys Acta. 2014;1843(8):1489-96. doi: 10.1016/j.bbamcr.2013.12.022. PubMed PMID: 24418623.

36. Chiba S, Lamsa A, Pogliano K. A ribosome-nascent chain sensor of membrane protein biogenesis in *Bacillus subtilis*. EMBO J. 2009;28(22):3461-75. Epub 2009/09/26. doi: 10.1038/emboj.2009.280. PubMed PMID: 19779460; PubMed Central PMCID: PMCPMC2782093.

37. Chen Y, Soman R, Shanmugam SK, Kuhn A, Dalbey RE. The role of the strictly conserved positively charged residue differs among the Gram-positive, Gram-negative, and chloroplast YidC homologs. J Biol Chem. 2014;289(51):35656-67. Epub 2014/11/02. doi: 10.1074/jbc.M114.595082. PubMed PMID: 25359772; PubMed Central PMCID: PMCPMC4271247.

38. Luo Y, Asai K, Sadaie Y, Helmann JD. Transcriptomic and phenotypic characterization of a *Bacillus subtilis* strain without extracytoplasmic function sigma factors. J Bacteriol. 2010;192(21):5736-45. Epub 2010/09/08. doi: 10.1128/JB.00826-10. PubMed PMID: 20817771; PubMed Central PMCID: PMCPMC2953670.

39. Zhao H, Sun Y, Peters JM, Gross CA, Garner EC, Helmann JD. Depletion of Undecaprenyl Pyrophosphate Phosphatases Disrupts Cell Envelope Biogenesis in *Bacillus subtilis*. J Bacteriol. 2016;198(21):2925-35. doi: 10.1128/JB.00507-16. PubMed PMID: 27528508; PubMed Central PMCID: PMCPMC5055597.

40. Hartl B, Wehrl W, Wiegert T, Homuth G, Schumann W. Development of a new integration site within the *Bacillus subtilis* chromosome and construction of compatible expression cassettes. J Bacteriol. 2001;183(8):2696-9. Epub 2001/03/29. doi: 10.1128/JB.183.8.2696-2699.2001. PubMed PMID: 11274134; PubMed Central PMCID: PMCPMC95191.

41. Koo BM, Kritikos G, Farelli JD, Todor H, Tong K, Kimsey H, et al. Construction and Analysis of Two Genome-Scale Deletion Libraries for *Bacillus subtilis*. Cell Syst. 2017;4(3):291-305 e7. Epub 2017/02/13. doi: 10.1016/j.cels.2016.12.013. PubMed PMID: 28189581; PubMed Central PMCID: PMCPMC5400513.
42. Rojas-Tapias DF, Helmann JD. Induction of the Spx regulon by cell wall stress reveals novel regulatory mechanisms in *Bacillus subtilis*. Mol Microbiol. 2018;107(5):659-74. Epub 2017/12/23. doi: 10.1111/mmi.13906. PubMed PMID: 29271514; PubMed Central PMCID: PMCPMC5820111.
43. Altenbuchner J. Editing of the *Bacillus subtilis* Genome by the CRISPR-Cas9 System. Appl Environ Microbiol. 2016;82(17):5421-7. Epub 2016/06/28. doi: 10.1128/AEM.01453-16. PubMed PMID: 27342565; PubMed Central PMCID: PMCPMC4988203.
44. Moszer I, Rocha EP, Danchin A. Codon usage and lateral gene transfer in *Bacillus subtilis*. Curr Opin Microbiol. 1999;2(5):524-8. Epub 1999/10/06. PubMed PMID: 10508724.
45. Schindelin J, Arganda-Carreras I, Frise E, Kaynig V, Longair M, Pietzsch T, et al. Fiji: an open-source platform for biological-image analysis. Nat Methods. 2012;9(7):676-82. Epub 2012/06/30. doi: 10.1038/nmeth.2019. PubMed PMID: 22743772; PubMed Central PMCID: PMCPMC3855844.
46. Zhao H, Roistacher DM, Helmann JD. Aspartate deficiency limits peptidoglycan synthesis and sensitizes cells to antibiotics targeting cell wall synthesis in *Bacillus subtilis*. Mol Microbiol. 2018;109(6):826-44. Epub 2018/07/12. doi: 10.1111/mmi.14078. PubMed PMID: 29995990; PubMed Central PMCID: PMCPMC6185803.
47. Radeck J, Kraft K, Bartels J, Cikovic T, Durr F, Emenegger J, et al. The *Bacillus* BioBrick Box: generation and evaluation of essential genetic building blocks for standardized work with Bacillus subtilis. J Biol Eng. 2013;7(1):29. Epub 2013/12/04. doi: 10.1186/1754-1611-7-29. PubMed PMID: 24295448; PubMed Central PMCID: PMCPMC4177231.
48. Pettersen EF, Goddard TD, Huang CC, Couch GS, Greenblatt DM, Meng EC, et al. UCSF Chimera--a visualization system for exploratory research and analysis. J Comput Chem. 2004;25(13):1605-12. Epub 2004/07/21. doi: 10.1002/jcc.20084. PubMed PMID: 15264254.

Figure Legends

Fig. 1. Identification of a SpoIIIJ variant that is necessary and sufficient to abolish the essentiality of the anti-σ^M factor YhdL. (A) Growth of PY79 P_M-*lacZ yhdL* strain on LB plate with 60 μg/ml X-Gal. (B) Transformation plate using 168 P_M-*lacZ* as recipient and PY79 P_M-*lacZ yhdL*::*kan* as DNA donor, with LB medium supplemented with kanamycin and X-Gal. Red arrows are pointed at intermediate sized blue colonies that were further analyzed by whole genome re-sequencing. (C) Alignment of YidC homologs from bacterial and eukaryotic species. Region of the Q140 of *B. subtilis* SpoIIIJ is shown. (D) Spot dilution of *yhdL* P_{xylA}-*yhdL* depletion strain with different SpoIIIJ alleles. WT168 has $SpoIIIJ^{Q140}$ allele. (E) Representative phase contrast microscopy image of *yhdL* mutants in different strain backgrounds. PY79 WT has $SpoIIIJ^{K140}$ allele. (F) Representative phase contrast microscopy photo of *yhdK* mutants in different strain backgrounds. (G) Colony morphology and size of *yhdK* mutants in different backgrounds. Colony size data were plotted using Box and Whisker chart and the bottom and top of the box are the first and third quartiles, the band inside the box is the second quartile (the median), and the X inside the box is the mean. Whiskers are one standard deviation above or below the mean. Outliers are shown as single dots. Average colony size change was calculated using formulation "change = (sample - control) / control x 100%". P value was calculated using student's t test, two tails, assuming unequal variances. Sample number n is at least 100 for each sample.

Fig. 2. Overexpression of SpoIIIJ increases tolerance of high σ^M activity. (A) Colony size of *yhdK* mutants in 168 background with overexpression of YidC homologs using an IPTG inducible $P_{spac(hy)}$ promoter. Cells were grown on LB plate supplemented with 1 mM IPTG for 24 hours at 37 °C. Box and Whisker chart was plotted as in Fig. 1G. (B) Representative Western blot of SpoIIIJ protein in different strain backgrounds. $P_{spac(hy)}$ and P_{xylA} induced SpoIIIJ strains contain the native SpoIIIJ and were induced with 1 mM IPTG or 1% (w/v) xylose, respectively. Part of the SDS PAGE gel was shown as a loading control. Relative SpoIIIJ quantity was

818 calculated using band intensity values from three biological replicates and normalized using total
819 lane intensity from the SDS PAGE gel. Data is presented as mean ± SEM.
820
821 **Fig. 3. Effects of different charge variants inside the SpoIIIJ substrate binding groove**. (A)
822 Schematic drawing showing the extracellular, transmembrane and cytoplasmic domains of
823 SpoIIIJ. The native sequence in strain 168 of the seven residues for the positive charge library
824 were shown. (B) Spot dilution of *yidC2* P_{xylA}-*yidC2* depletion strain with different SpoIIIJ
825 variants in strain 168. (C) Colony size of *yhdK spoIIIJ* mutants with different *spoIIIJ* alleles
826 integrated in *thrC* site. Residues that provide positive charge(s), as well as total positive
827 charge(s) provided by these seven variable positions are labelled. The red line shows the median
828 of colony size with a WT SpoIIIJ from strain 168. Box and Whisker chart was plotted as in Fig.
829 1G. (D) Top, representative Western blots of SpoIIIJ protein in different strain backgrounds. Part
830 of the SDS PAGE gels were shown as loading control. Bottom, activity of *yidC2*'-*lacZ*
831 translational fusion in the same strain backgrounds of the Western blots. "WT" has a native copy
832 of *spoIIIJ* while "*spoIIIJ*" is a markerless deletion mutant. All other strains have the native
833 *spoIIIJ* deleted and contain variants of *spoIIIJ* at *thrC* site. Among the seven variable positions,
834 residues that provide positive charge(s) are labelled. SpoIIIJ variants inside the red boxes cannot
835 support growth of a *yidC2* P_{xylA}-*yidC2* depletion strain in the absence of inducer xylose. Green
836 shading highlights the difference between the activity of SpoIIIJ at the native and *thrC* loci.
837 Variants with *yidC2*'-*lacZ* activity inside the green shading exhibit increased MifM insertion
838 activity compared with WT.
839
840 **Fig. 4. High σ^M activity causes a cascade of stresses that can be partially compensated by its**
841 **own regulon**. (A) Maximum promoter activity of *htrA* measured using a P_{htrA}-*lux* transcriptional
842 fusion reporter in different strain backgrounds. Data is presented as mean ± SEM, and
843 statistically significant different samples (Student's t test, two-tailed $P<0.05$) are labelled with
844 different letters. Sample number n is at least 4. (B) Colony size of *yhdK* mutants in strain 168
845 with different additional mutations. Box and Whisker chart was plotted as in Fig. 1G. (C) Fold
846 change of transcription levels of representative genes for stress response or housekeeping genes.
847 Data is presented as mean ± SEM. Sample number n is at least 4. (D) Colony size of *yhdK*
848 mutants in strain 168 with different additional mutations. ΔP_M-*spx* strain has the native *spx*

deleted and an ectopic copy without the P_M promoter [42]. (E) Schematic drawing of *maf, murG* operon and *rodA* gene. σ^A and σ^M controlled promoters are shown with arrows. Cytoplasmic proteins are labelled in blue boxes, peripheral membrane proteins in pink boxes, and membrane integral proteins in red boxes. (F, G) Colony size of *yhdK* mutants with different P_M promoter(s) mutated in (F) WT strain 168 or (G) strain 168 with the native *spoIIIJ* deleted and a SpoIIIJ^{Q140K} allele integrated at the *thrC* site. Box and Whisker chart was plotted as in Fig. 1G.

Supplemental Figure legends

Fig. S1. **A**. Map of SNPs from strain PY79 to 168 and distribution of SNPs contained in each congression suppressors. Genome coordinates were based on the 168 reference genome with NCBI accession number NC_000964.3. **B**. Transformation plates of *yhdL*::*kan* allele transformed into different strain backgrounds, selected on LB plates supplemented with kanamycin, X-gal and 1% xylose. **C**. Variation of *yhdK* colony size measurement between trials on different days with different batches of LB plates. P value was calculated using Student's t test, and percentage changes of average colony size were shown.

Fig. S2. A. Venn diagram of function overlap and distinction of SpoIIIJ and YidC2 of *Bacillus subtilis*. **B**. Streaking of *yhdK* $P_{spac(hy)}$-*yidC2*^{Q148K} on plates of LB or LB supplemented with 1 mM IPTG (final concentration). **C**. Spot dilution of *yhdL* depletion strains with $P_{spac(hy)}$ based overexpression of different YidC homologs, on LB plates supplemented with a final concentration of 1% xylose (+Xylose), 1 mM IPTG (+IPTG) or nothing (None).

Fig. S3. A. Distribution of 128 possible charges of SpoIIIJ in the *spoIIIJ* variants library. Theoretically, the majority of SpoIIIJ in the input DNA library contains +2 to +5 charges, while experimental data from 103 samples suggests the ones capable of providing high SigM tolerance contain +2 or +3 charges. Among the 103 samples with +2 or +3 charges, the positive charge can be located in one, two or three transmembrane segments, with the exception that no sample contains more than one positive charge in TM1 alone. **B**. Crystal structure of YidC from *Bacillus halodurans* (PDB ID 3WO6), showing the seven variable amino acid providing positive charges in the hydrophilic substrate binding chamber of the enzyme. Gly231 is not visible due to the lack

of side chain of this residue. TM1-5, transmembrane region 1-5; E1, extracytoplasmic region 1; C1, cytoplasmic region 1.This figure was generated using UCSF Chimera 1.13[48]. **C**. Streaking of *yhdL* depletion strains with SpoIIIJ variants on LB plates with or without xylose inducer for *yhdL*. The positive charge of each variant was labelled next to the streaking, with a negative control "None" meaning no *spoIIIJ* variants at *thrC* locus (weak growth due to the depletion conditions, and cannot be restreaked), and a positive control "$SpoIIIJ_{PY79}$" meaning the native SpoIIIJ mutated into the PY79 Q140K version (HB23719). **D**. Spot dilution of YidC depletion strains with *spoIIIJ* variants at *thrC* locus. The depletion strain has its native *spoIIIJ* and *yidC2* deleted, and a xylose inducible copy of P_{xylA}-*yidC2*. Diluted cultures were spotted on LB without xylose (-Xyl) or with 1% final concentration of xylose (+Xyl). The negative control (None) has no *spoIIIJ* at *thrC* locus, while the positive control has the 168 version of *spoIIIJ* that contains a single positive charge at R73. Some SpoIIIJ variants exhibited reduced growth ability, and the variant containing R72 K140 R144 failed to growth, although the emergence of suppressors was noted.

Fig. S4. Colony size of different strains. Percentage changes of average colony size were shown on each Box and Whisker plot.

Table S1. Genes compared between reference genomes of *B. subtilis* 168 (NCBI accession number NC_000964.3) and PY79 (NC_022898.1). No mutations were found in these genes.

Table S2. Whole genome sequencing of transformants generated by congression.

Table S3. Amino acid substitutions in SpoIIIJ variants selected in *yhdL* depletion strain.

Table S4. Secreted and membrane-associated proteins in the σ^M regulon.

Table S5. *Bacillus subtilis* strains used in this study.

Table S6. Primers used in this study.

Figure 1. Identification of a SpoIIIJ mutant that is necessary and sufficient to abolish the essentiality of the anti-SigM factor YhdL

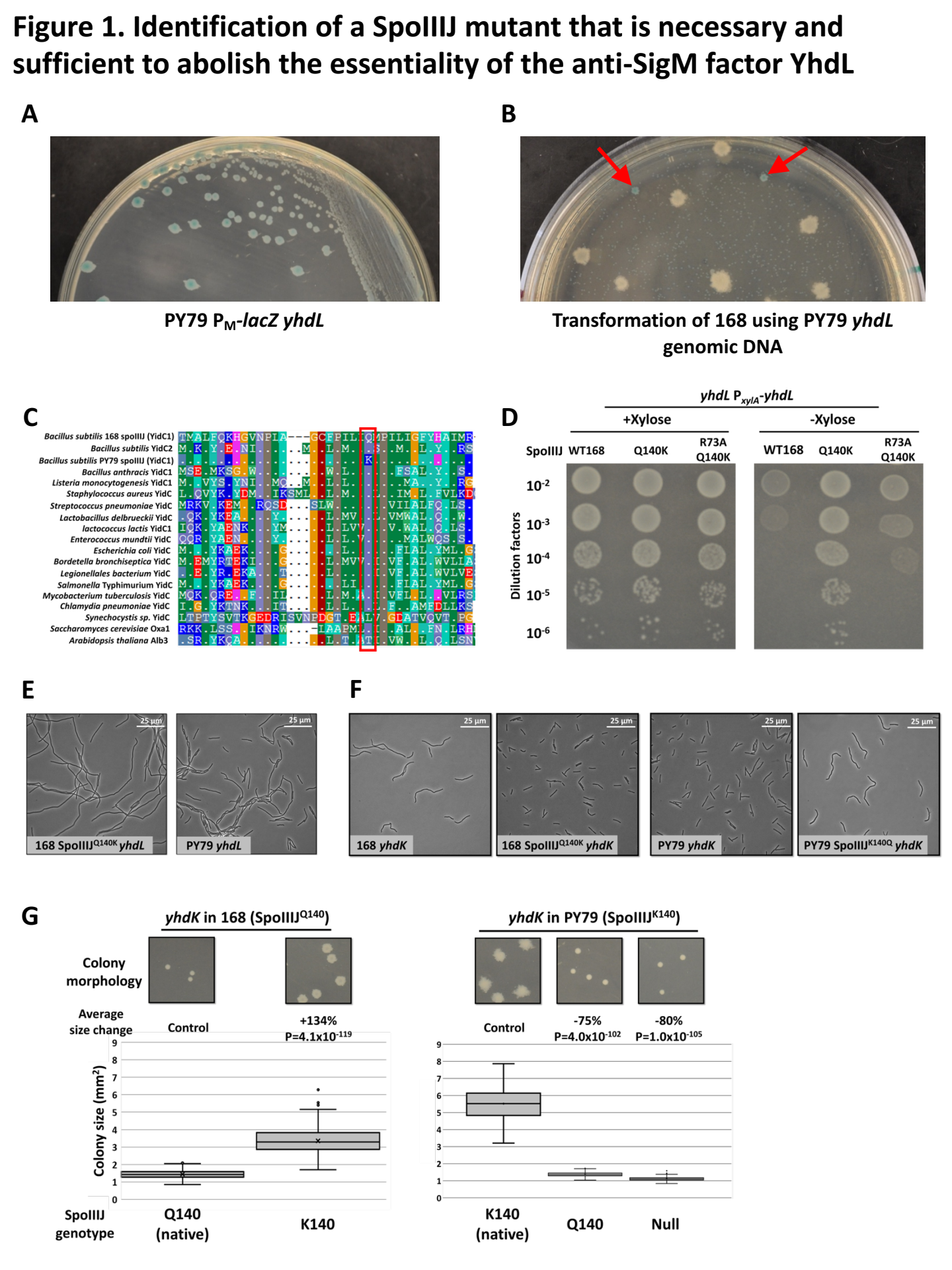

Figure 2. Overexpression of SpoIIIJ increases tolerance of high σ^M activity.

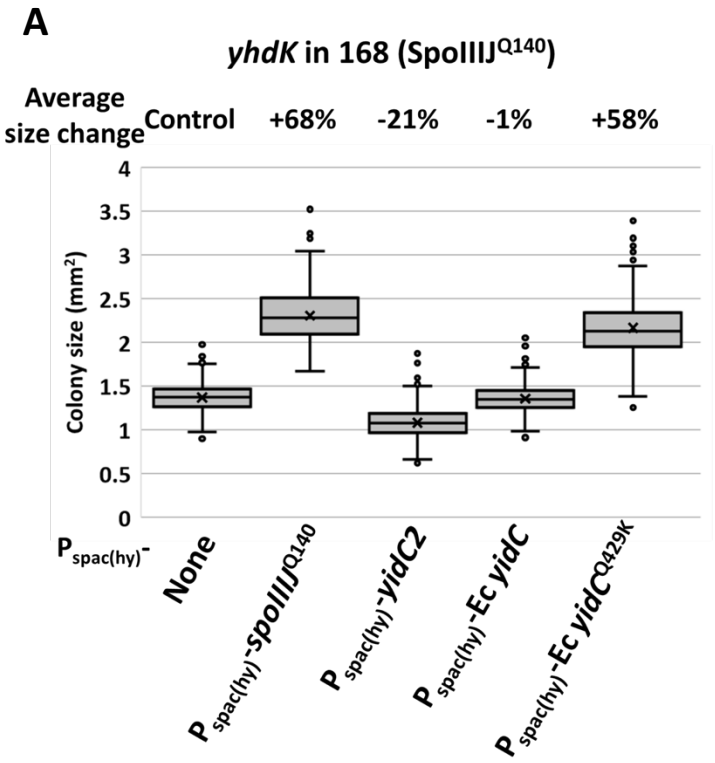

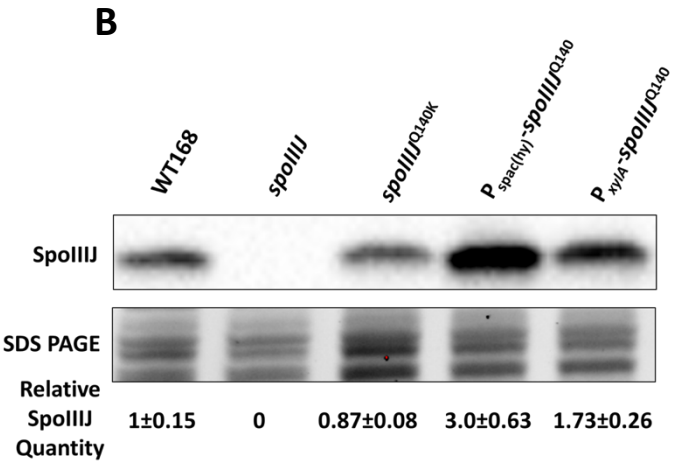

Figure 3. Effects of different charge variants inside the SpoIIIJ substrate binding groove

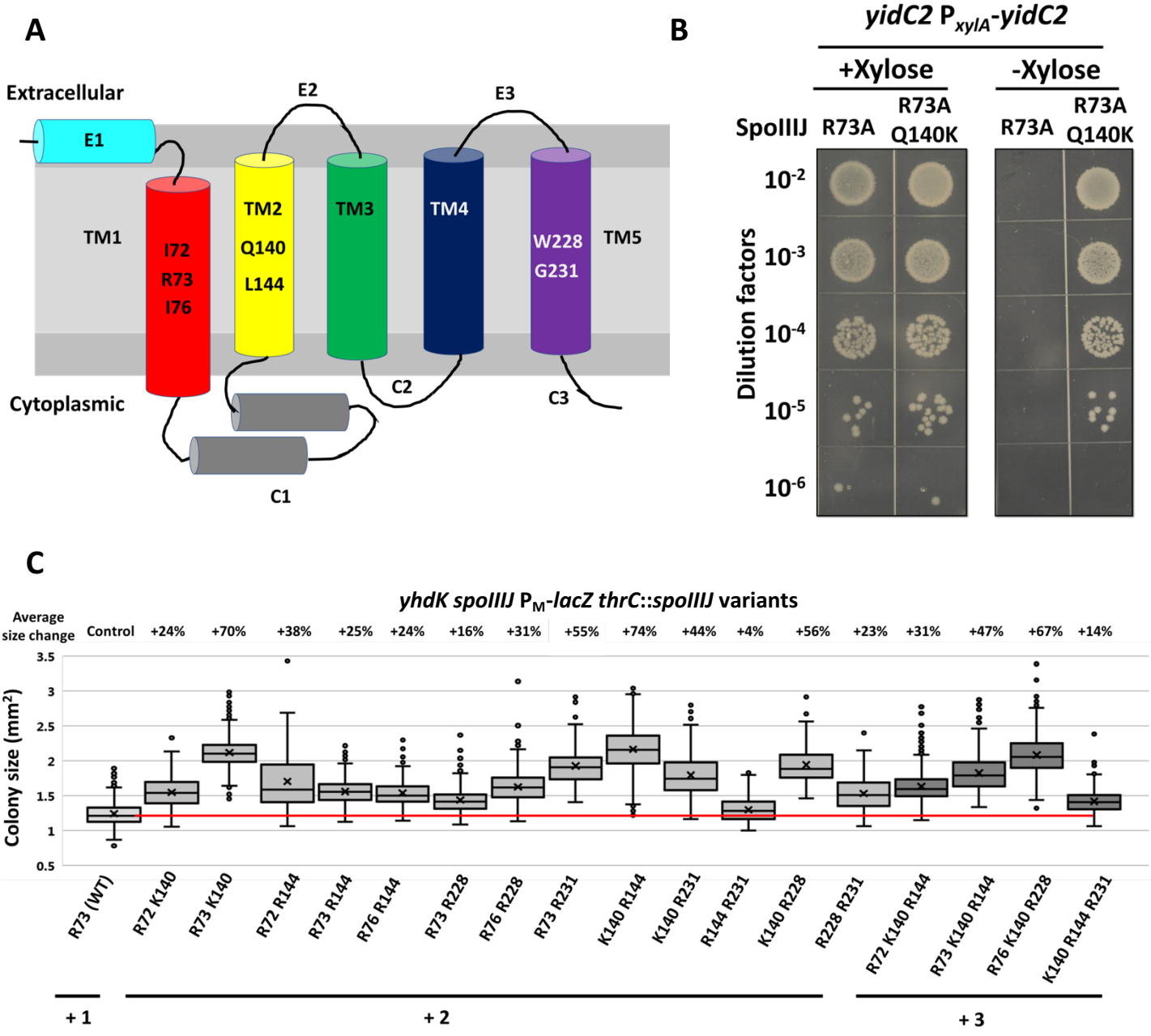

Figure 3. Effects of different charge variants inside the SpoIIIJ substrate binding groove

D

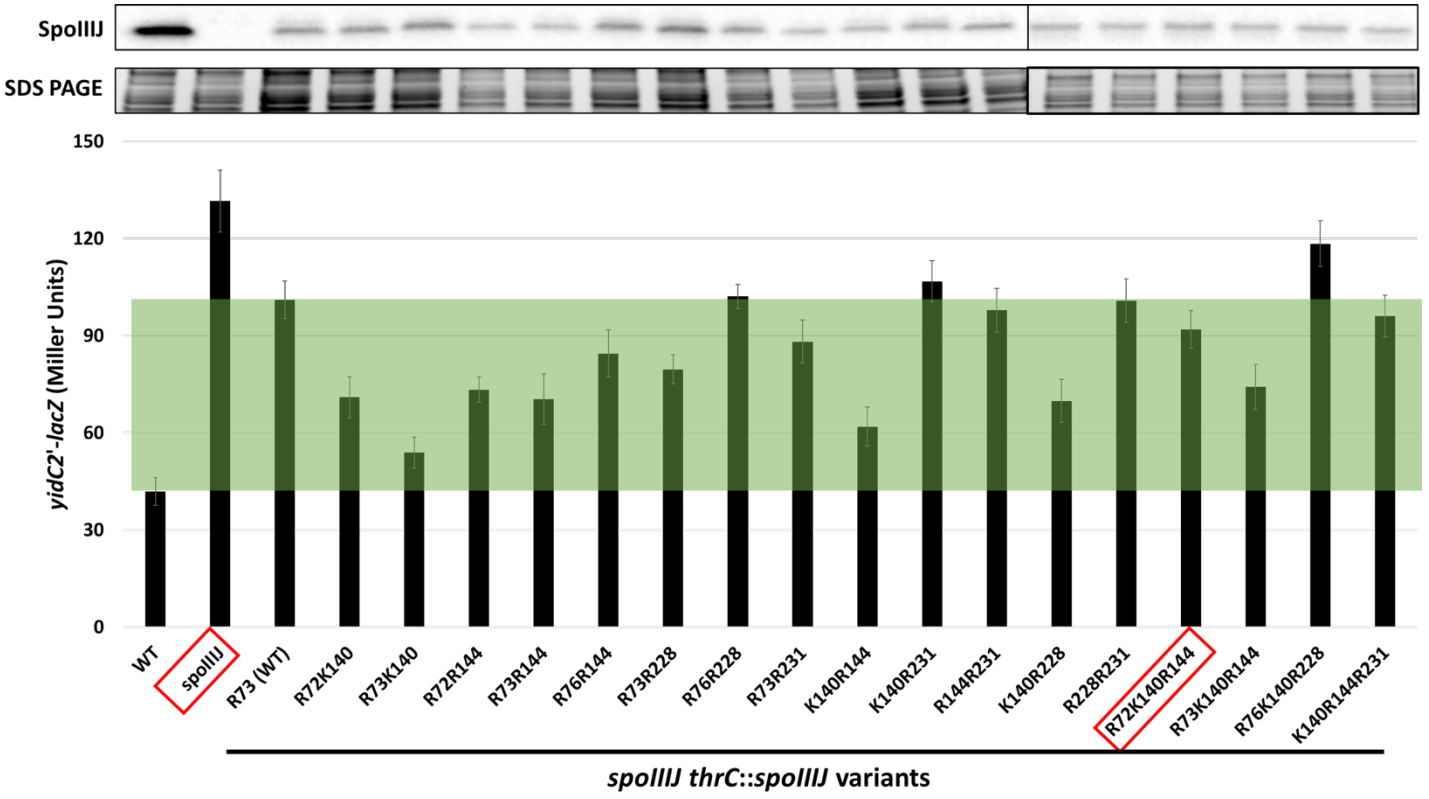

Figure 4. High σ^M activity causes a cascade of stresses that can be partially compensated by its own regulon

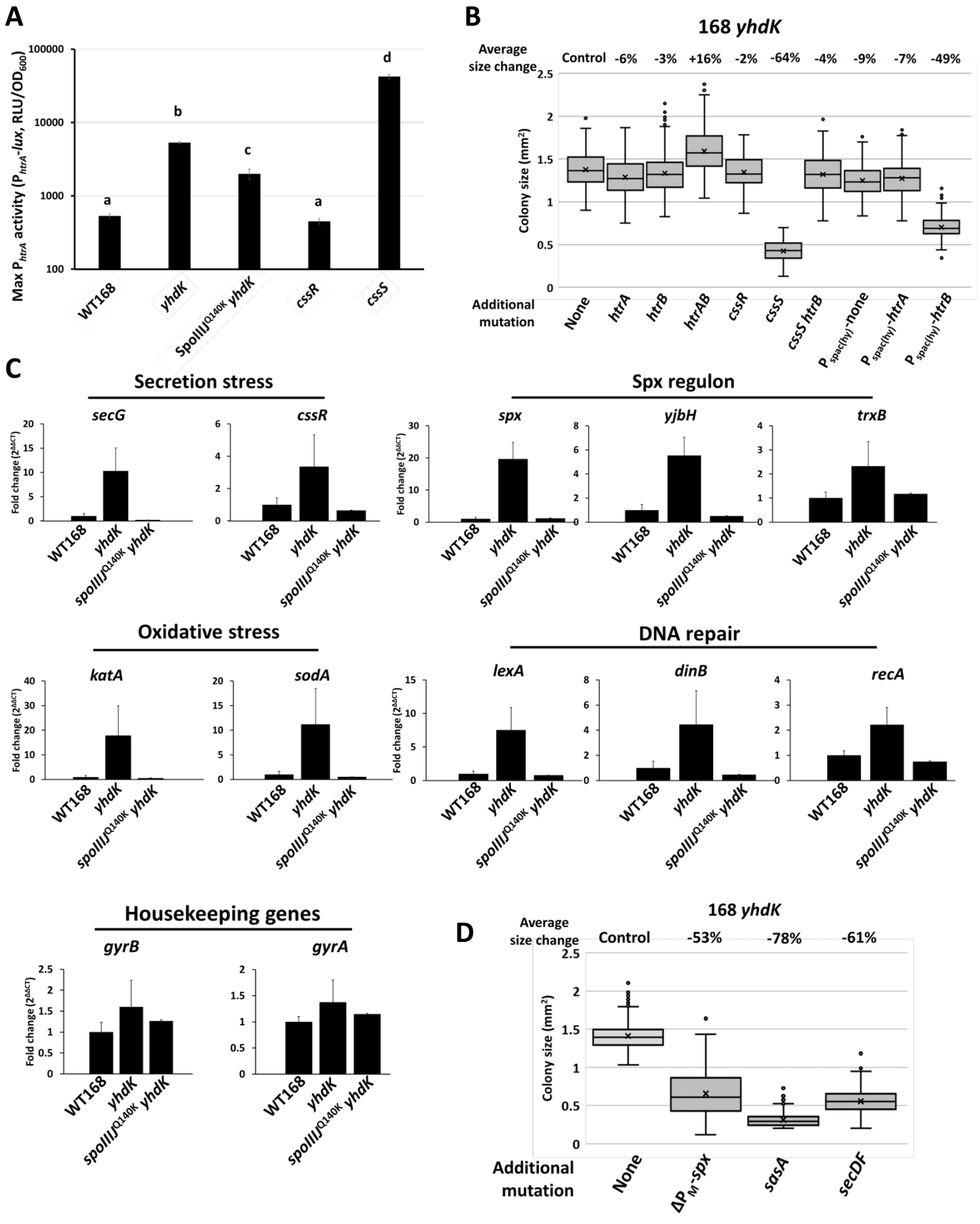

Figure 4. High SigM activity causes a cascade of stresses that can be partially compensated by its regulon

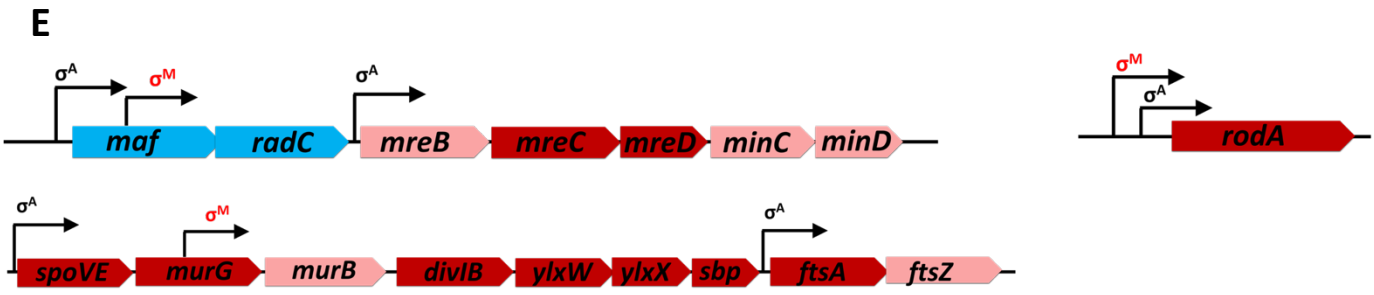

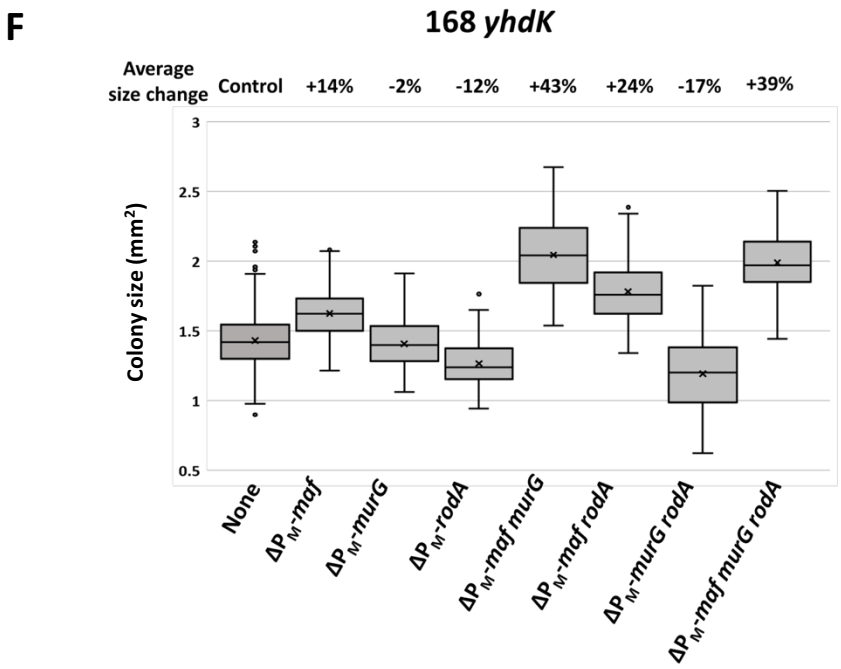

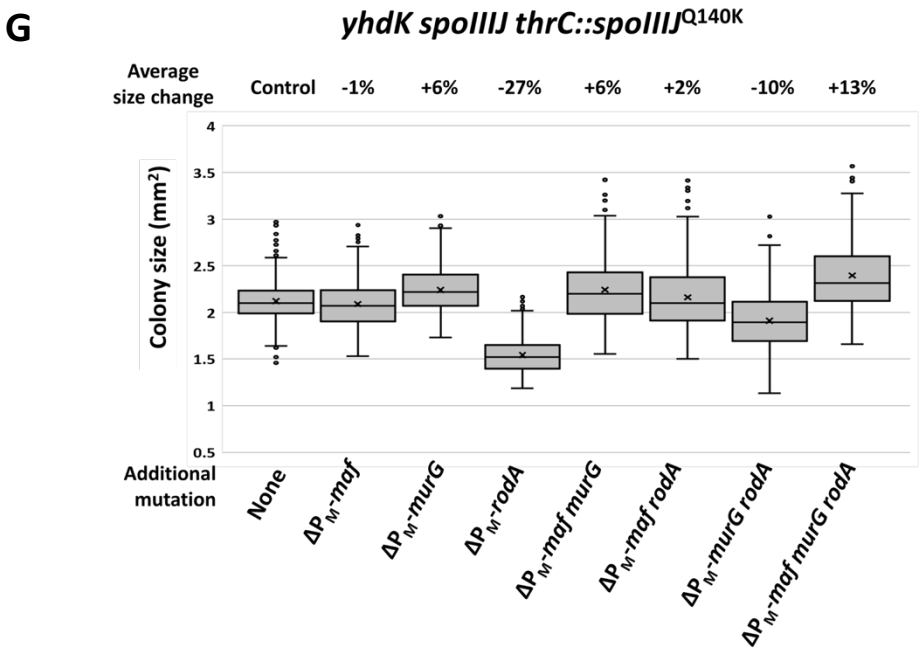

Figure S1

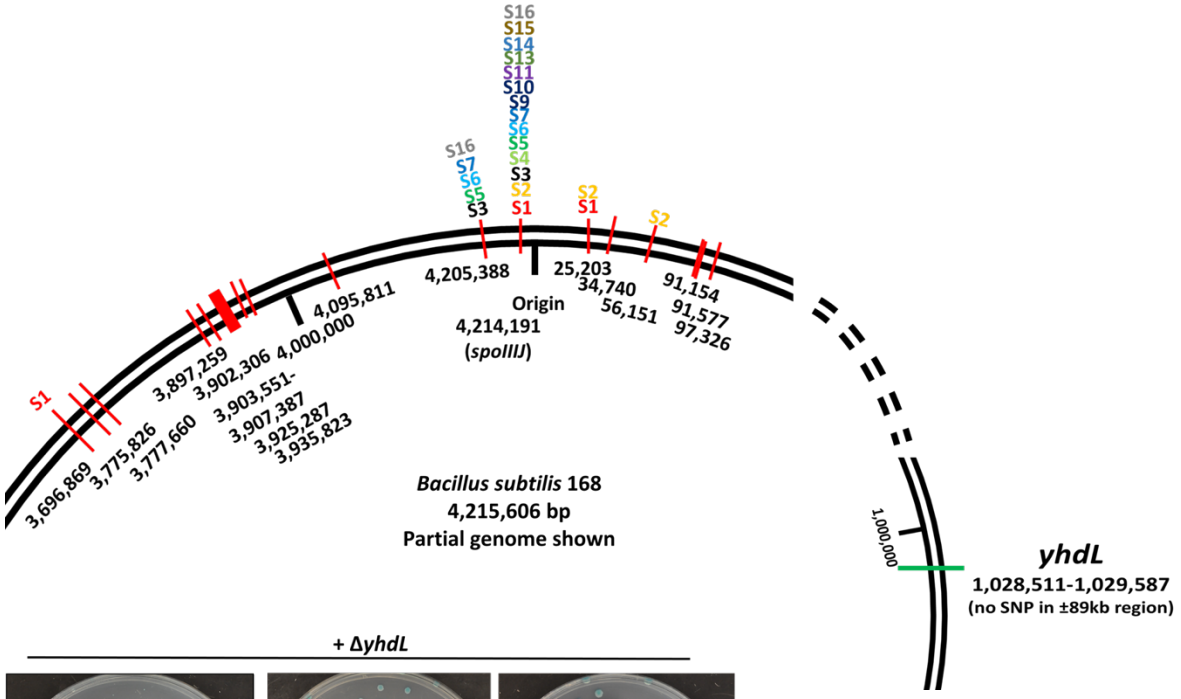
A
S16
S15
S14
S13
S11
S10
S9
S7
S6
S5
S4
S3
S2
S1
4,205,388
Origin
4,214,191
(spoIIIJ)
25,203
34,740
56,151
91,154
91,577
97,326
4,095,811
4,000,000
3,897,259
3,902,306
3,903,551-
3,907,387
3,925,287
3,935,823
3,696,869
3,775,826
3,777,660
1,000,000
Bacillus subtilis 168
4,215,606 bp
Partial genome shown
yhdL
1,028,511-1,029,587
(no SNP in ±89kb region)

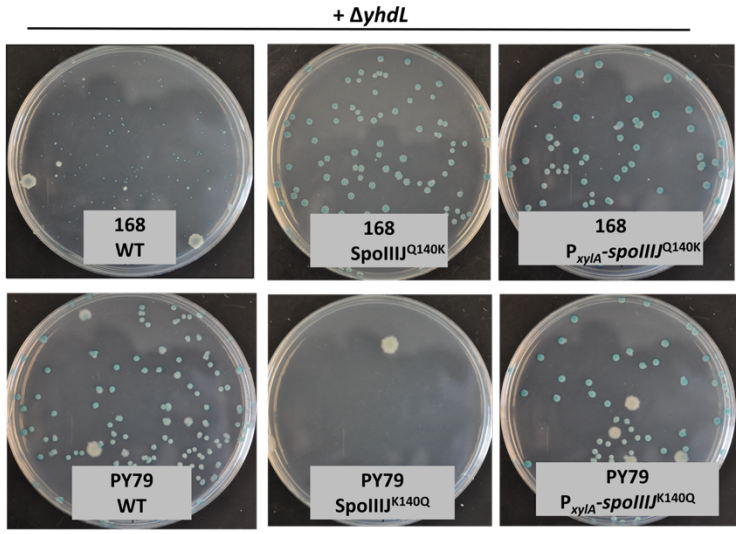
B
+ ΔyhdL
168 WT
168 SpoIIIJQ140K
168 PxylA-spoIIIJQ140K
PY79 WT
PY79 SpoIIIJK140Q
PY79 PxylA-spoIIIJK140Q

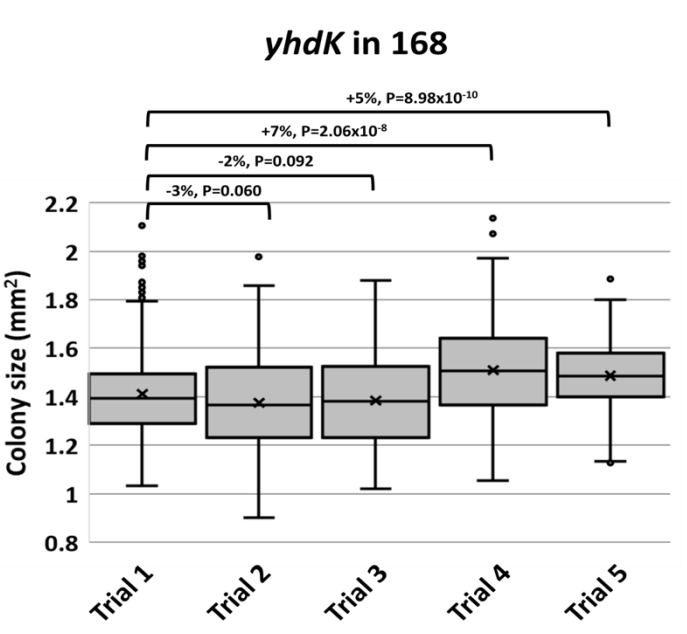
C
yhdK in 168
+5%, P=8.98x10-10
+7%, P=2.06x10-8
-2%, P=0.092
-3%, P=0.060
Colony size (mm2)
2.2
2
1.8
1.6
1.4
1.2
1
0.8
Trial 1
Trial 2
Trial 3
Trial 4
Trial 5

Figure S2

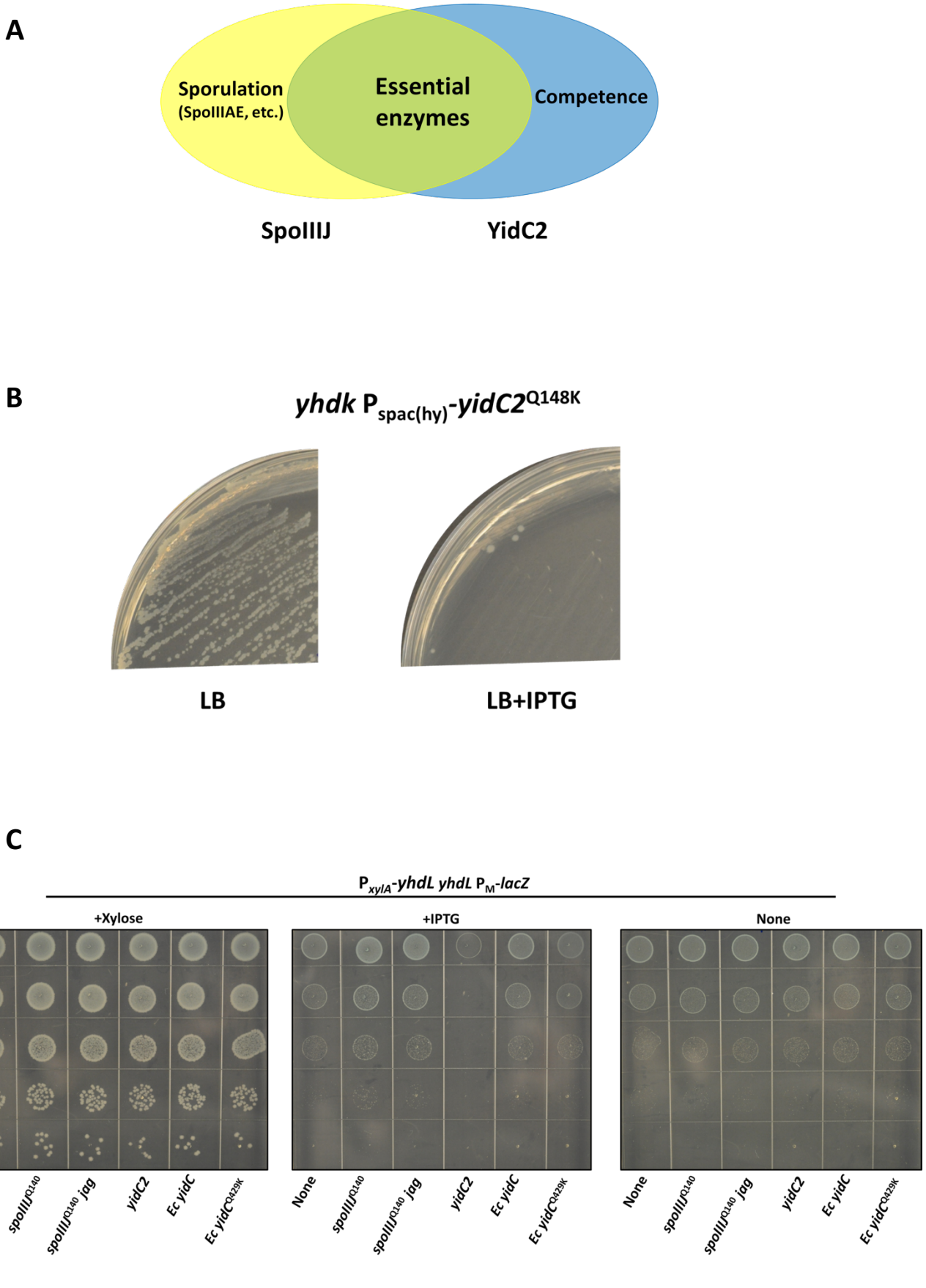
A
Sporulation
(SpoIIIAE, etc.)
Essential
enzymes
Competence
SpoIIIJ
YidC2
B
yhdk Pspac(hy)-yidC2Q148K
LB
LB+IPTG
C
PxylA-yhdL yhdL PM-lacZ
+Xylose
+IPTG
None
Dilution factors
10-1
10-2
10-3
10-4
10-5
Pspac(hy)-
None
spoIIIJQ140
spoIIIJQ140 jag
yidC2
Ec yidC
Ec yidCQ429K

Figure S3

A

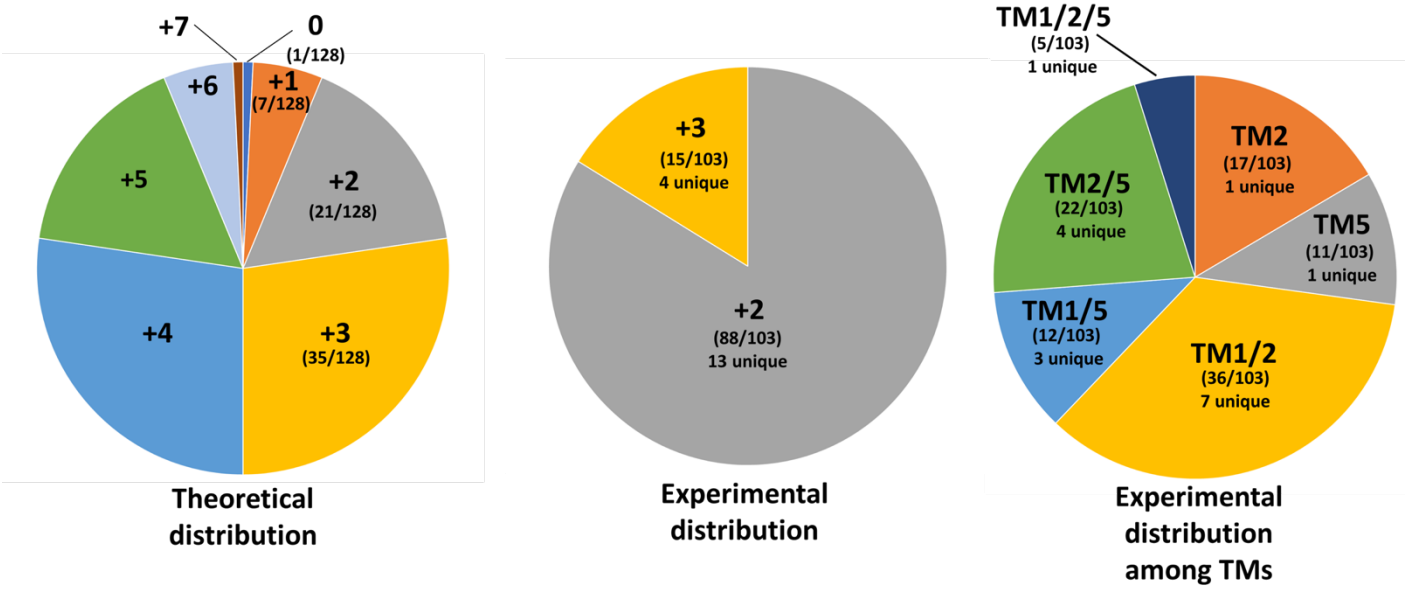
+7
0
(1/128)
+6
+1
(7/128)
+5
+2
(21/128)
+4
+3
(35/128)
Theoretical distribution
+3
(15/103)
4 unique
+2
(88/103)
13 unique
Experimental distribution
TM1/2/5
(5/103)
1 unique
TM2
(17/103)
1 unique
TM2/5
(22/103)
4 unique
TM5
(11/103)
1 unique
TM1/5
(12/103)
3 unique
TM1/2
(36/103)
7 unique
Experimental distribution among TMs

B

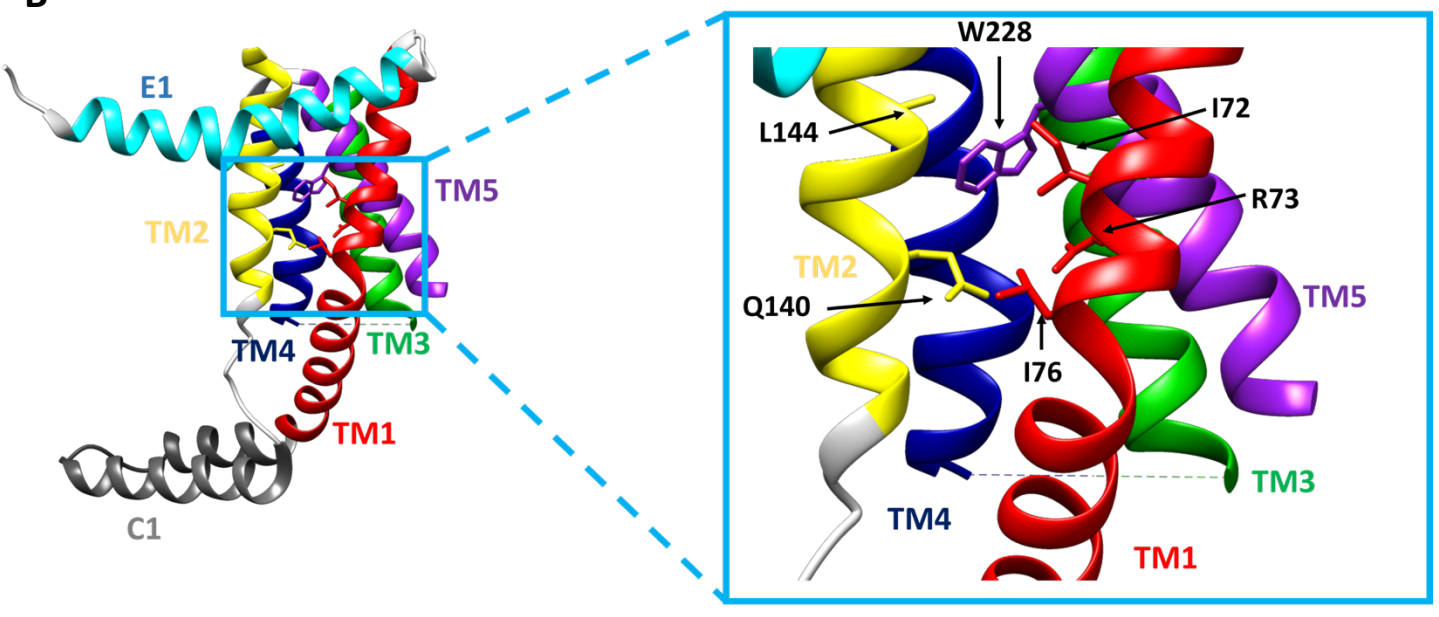
E1
TM5
TM2
TM4
TM3
TM1
C1
W228
L144
I72
R73
TM2
Q140
TM5
I76
TM3
TM4
TM1

Figure S3

C

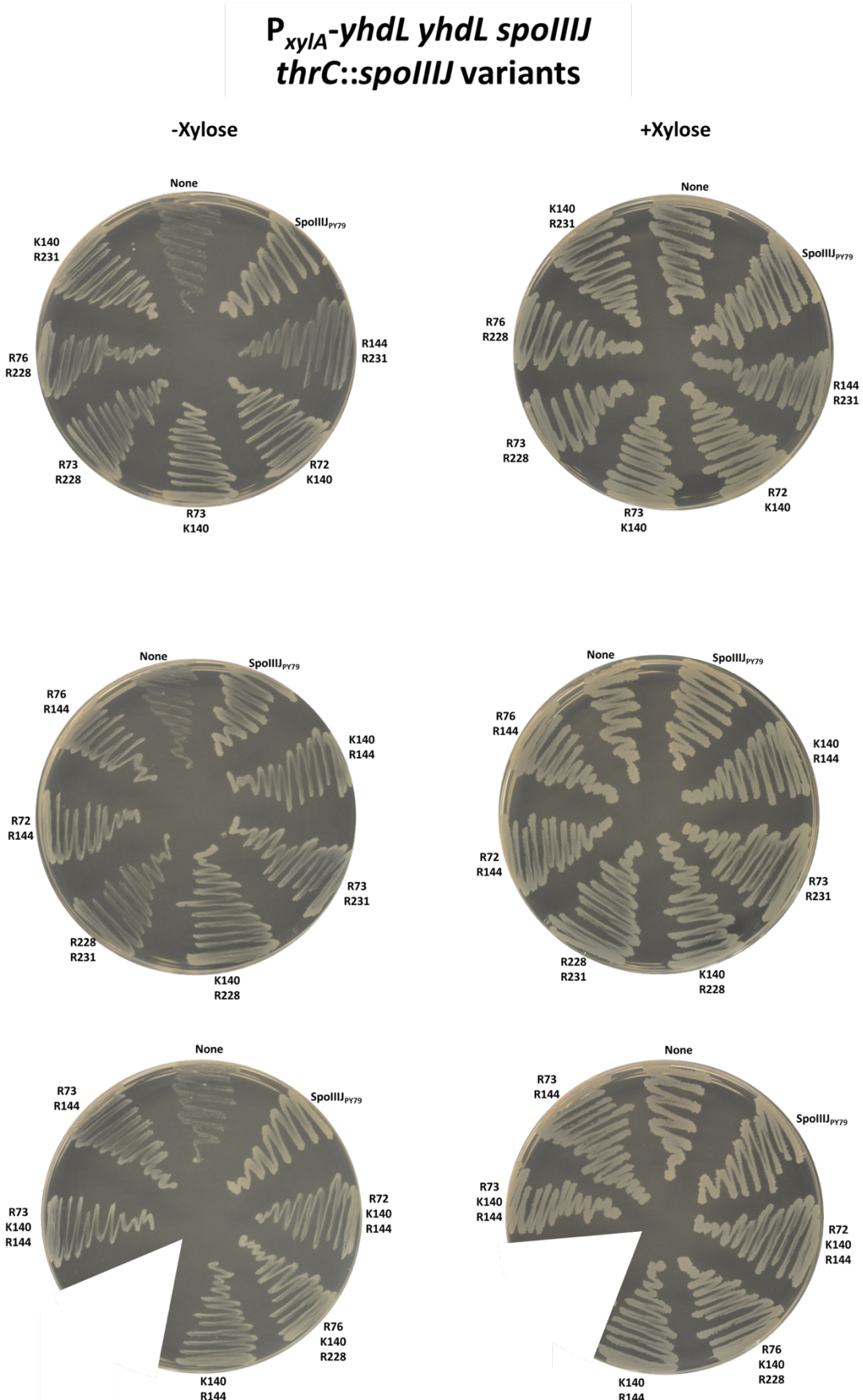
P xylA-yhdL yhdL spoIIIJ
thrC::spoIIIJ variants
-Xylose
+Xylose
None
SpoIIIJ PY79
K140 R231
R144 R231
R76 R228
R73 R228
R72 K140
R73 K140
None
SpoIIIJ PY79
K140 R231
R144 R231
R76 R228
R73 R228
R72 K140
R73 K140
None
SpoIIIJ PY79
R76 R144
K140 R144
R72 R144
R73 R231
R228 R231
K140 R228
None
SpoIIIJ PY79
R76 R144
K140 R144
R72 R144
R73 R231
R228 R231
K140 R228
None
SpoIIIJ PY79
R73 R144
R72 K140 R144
R73 K140 R144
R76 K140 R228
K140 R144
None
SpoIIIJ PY79
R73 R144
R72 K140 R144
R73 K140 R144
R76 K140 R228
K140 R144

Figure S3

D

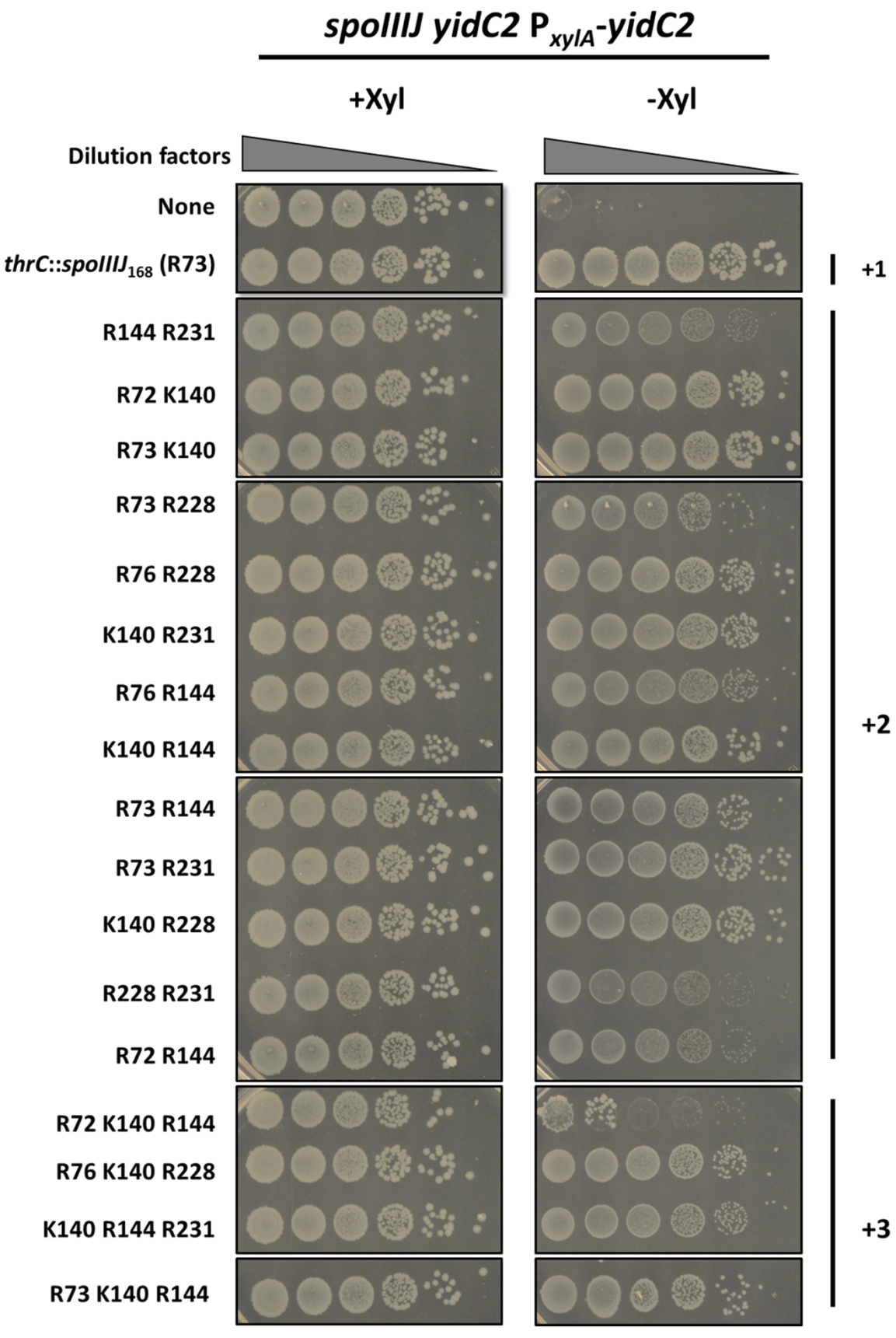
spoIIIJ yidC2 P$_{xylA}$-yidC2
+Xyl
-Xyl
Dilution factors
None
thrC::spoIIIJ$_{168}$ (R73)
R144 R231
R72 K140
R73 K140
R73 R228
R76 R228
K140 R231
R76 R144
K140 R144
R73 R144
R73 R231
K140 R228
R228 R231
R72 R144
R72 K140 R144
R76 K140 R228
K140 R144 R231
R73 K140 R144
+1
+2
+3

Figure S4

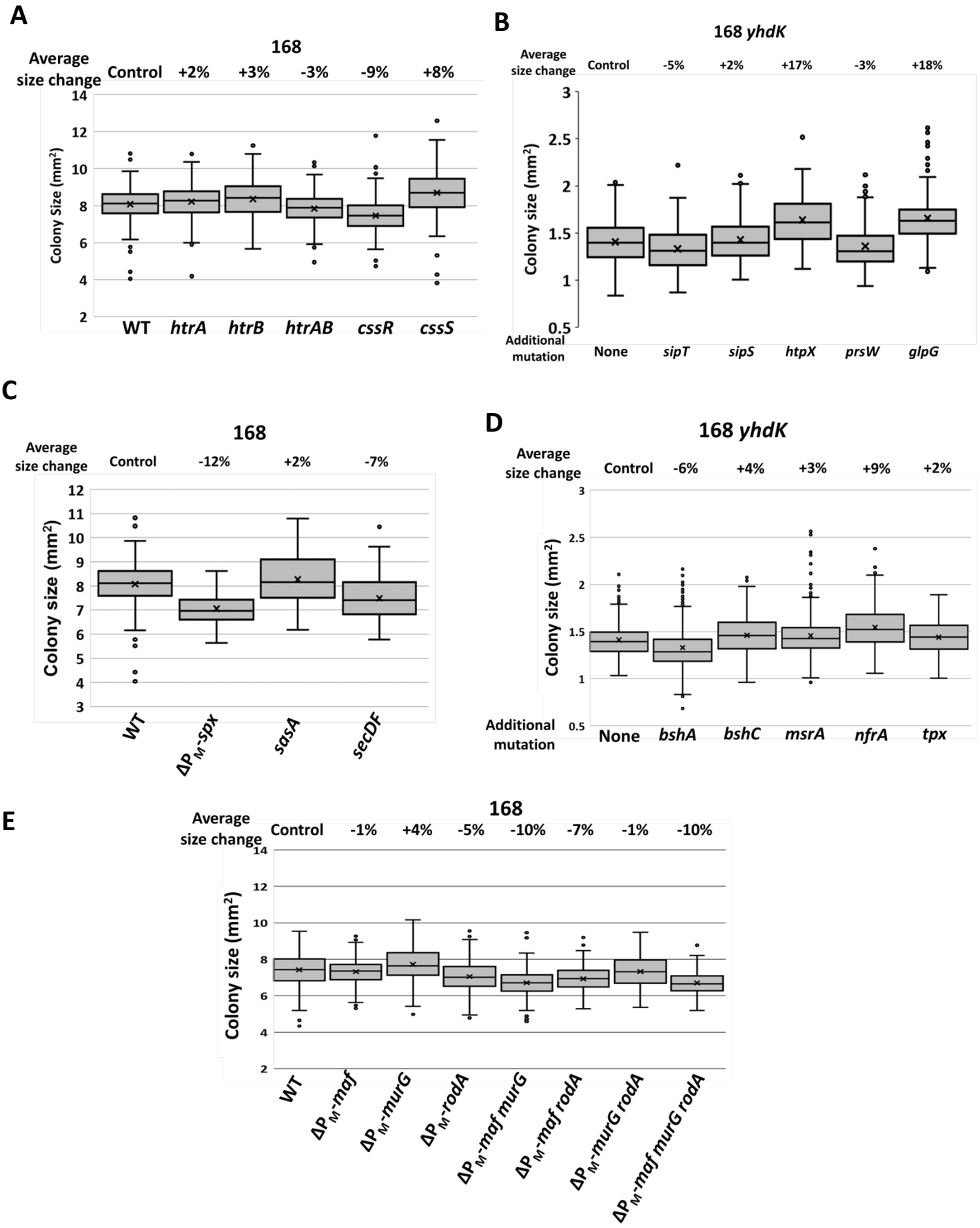
A
168
Average size change
Control
+2%
+3%
-3%
-9%
+8%
Colony Size (mm²)
WT
htrA
htrB
htrAB
cssR
cssS
B
168 yhdK
Average size change
Control
-5%
+2%
+17%
-3%
+18%
Colony size (mm²)
Additional mutation
None
sipT
sipS
htpX
prsW
glpG
C
168
Average size change
Control
-12%
+2%
-7%
Colony size (mm²)
WT
ΔPM-spx
sasA
secDF
D
168 yhdK
Average size change
Control
-6%
+4%
+3%
+9%
+2%
Colony size (mm²)
Additional mutation
None
bshA
bshC
msrA
nfrA
tpx
E
168
Average size change
Control
-1%
+4%
-5%
-10%
-7%
-1%
-10%
Colony size (mm²)
WT
ΔPM-maf
ΔPM-murG
ΔPM-rodA
ΔPM-maf murG
ΔPM-maf rodA
ΔPM-murG rodA
ΔPM-maf murG rodA

Table S1. Genes compared between reference genomes of *B. subtilis* 168 (NCBI accession number NC_000964.3) and PY79 (NC_022898.1). No SNP was found in these genes.

Accession Number	Gene
RNAP subunits	
BSU01430	*rpoA*
BSU01070	*rpoB*
BSU01080	*rpoC*
BSU37160	*rpoE*
BSU14540	*rpoY*
BSU15690	*rpoZ*
SigM regulon	
BSU00700	*coaX*
BSU00620	*divIC*
BSU00880	*disA*
BSU38500	*dltA*
BSU38510	*dltB*
BSU38520	*dltC*
BSU38530	*dltD*
BSU38540	*dltE*
BSU00690	*ftsH*
BSU00680	*hprT*
BSU21910	*metA*
BSU28000	*minC*
BSU27990	*minD*
BSU28030	*mreB*
BSU28020	*mreC*
BSU28010	*mreD*
BSU16950	*pbpX*
BSU36380	*rapD*
BSU27650	*secDF*
BSU35650	*tagU*
BSU00670	*tilS*
BSU21920	*ugtP*
BSU00710	*yacC*
BSU00890	*yacL*
BSU00900	*ispD*
BSU02890	*yceC*
BSU02900	*yceD*
BSU02910	*yceE*
BSU02920	*yceF*
BSU02930	*yceG*
BSU02940	*yceH*
BSU03240	*ycgQ*
BSU03250	*ycgR*
BSU04230	*ydaH*
BSU04560	*ddl*
BSU04570	*murF*
BSU06380	*yebC*
BSU07260	*yfnI*
BSU09500	*yhdK*
BSU09510	*yhdL*
BSU09520	*sigM*
BSU11490	*yjbC*
BSU11500	*spx*
BSU14480	*abh*
BSU15230	*murB*
BSU15240	*divIB*
BSU15250	*ylxW*
BSU15260	*ylxX*
BSU15270	*sbp*
BSU18190	*yngC*
BSU22310	*recU*
BSU22320	*ponA*
BSU22980	*ypbG*
BSU23300	*ypuD*
BSU23370	*ypuA*
BSU23830	*yqjL*
BSU27180	*yrhH*
BSU27160	*yrhJ*
BSU27170	*fatR*
BSU28040	*radC*
BSU30500	*ytpB*
BSU30510	*ytpA*
BSU35840	*tagT*
BSU36530	*bcrC*
BSU38120	*rodA*
BSU38480	*ywaC*
BSU38260	*ywbN*
BSU38250	*ywbO*
BSU36540	*ywnJ*
Spx regulon	
BSU00730	*cysK*
BSU14710	*ylaA*
BSU14720	*ylaB*
BSU14730	*ylaC*
BSU14740	*ylaD*
BSU21680	*msrB*
BSU21690	*msrA*
BSU27240	*yrhC*
BSU27250	*mccB*
BSU27260	*mccA*
BSU27270	*mtnN*
BSU27280	*yrrT*
BSU28500	*trxA*
BSU29490	*tpx*
BSU31290	*yugT*
BSU31370	*yugJ*
BSU30340	*ytvA*
BSU34790	*trxB*
BSU38110	*nfrA*
BSU29820	*ytpR*
BSU29830	*ytpQ*
BSU29840	*ytpP*
BSU03480	*srfAA*
BSU03490	*srfAB*
BSU03500	*comS*
BSU03510	*srfAC*
BSU03520	*srfAD*

Table S2. Whole genome sequencing of transformants generated by congression

Position	Reference	Allele	Count	Coverage	Frequency	Gene	DNA change	Amino acid change
Supp-1								
25203	G	A	72	75	96			
96240	G	A	86	138	62.32			
96260	G	A	65	122	53.28			
486574	T	C	68	69	98.55	*ydaO*	143T>C	Ile48Thr
1297396	G	A	73	73	100	*yjlA*	199C>T	Pro67Ser
2277179	A	C	83	83	100	*yokI*	243T>G	Ile81Met
2277245	GT	AC	36	64	56.25	*yokI*	176_177delACinsGT	Asp59Gly
3391676	A	G	41	41	100	*gerAA*	895A>G	Thr299Ala
3696869	T	C	97	97	100	*pgdS*	630A>G	
4214191	G	T	63	63	100	*spoIIIJ*	418C>A	Gln140Lys
Supp-2								
25203	G	A	61	61	100			
56151	G	A	67	67	100	*spoVG*	286G>A	Ala96Thr
455105	T	C	14	25	56	*yczH*	156A>G	
4214191	G	T	50	50	100	*spoIIIJ*	418C>A	Gln140Lys

Position	Reference	Allele	Count	Coverage	Frequency	Gene	DNA change	Amino acid change
Supp-3								
4205388	G	A	101	101	100	*yyaC*	489G>A	
4214191	G	T	60	60	100	*spoIIIJ*	418C>A	Gln140Lys
Supp-4								
4214191	G	T	49	49	100	*spoIIIJ*	418C>A	Gln140Lys
Supp-5								
2600044	TATTGTATAATG	-	42	43	97.67			
4205388	G	A	79	79	100	*yyaC*	489G>A	
4214191	G	T	67	68	98.53	*spoIIIJ*	418C>A	Gln140Lys
Supp-6								
4205388	G	A	97	97	100	*yyaC*	489G>A	
4214191	G	T	67	69	97.1	*spoIIIJ*	418C>A	Gln140Lys

Position	Reference	Allele	Count	Coverage	Frequency	Gene	DNA change	Amino acid change
Supp-7								
4205388	G	A	72	72	100	*yyaC*	489G>A	
4214191	G	T	47	47	100	*spoIIIJ*	418C>A	Gln140Lys
Supp-9								
4214191	G	T	11	11	100	*spoIIIJ*	418C>A	
Supp-10								
4214191	G	T	51	51	100	*spoIIIJ*	418C>A	Gln140Lys
Supp-11								
2002473	T	G	85	87	97.7			
4214191	G	T	71	71	100	*spoIIIJ*	418C>A	Gln140Lys
Supp-12								
2707867	A	C	59	86	68.6			

Position	Reference	Allele	Count	Coverage	Frequency	Gene	DNA change	Amino acid change
Supp-13								
3810012	G	A	128	129	99.22			
4214191	G	T	47	47	100	*spoIIIJ*	418C>A	Gln140Lys
Supp-14								
96240	G	A	16	17	94.12			
96260	G	A	13	14	92.86			
775706	-	T	18	32	56.25	*yesZ*	907_908insT	Ala303fs
775707	C	T	18	32	56.25	*yesZ*	909C>T	
775710	-	T	17	33	51.52	*yesZ*	911_912insT	Leu305fs
775721	CC	AA	12	28	42.86	*yesZ*	923_924delCCinsAA	Ser308*
1013666	G	T	15	28	53.57	*nsrR*	186C>A	
1855412	A	T	17	34	50	*pksR*	4523A>T	Asn1508Ile
1855416	A	T	18	36	50	*pksR*	4527A>T	Gln1509His
1855428	T	G	21	40	52.5	*pksR*	4539T>G	Ile1513Met
2129223	G	C	37	37	100	*yodE*	771C>G	
2846430	T	A	11	21	52.38	*nadA*	632A>T	Glu211Val

Position	Reference	Allele	Count	Coverage	Frequency	Gene	DNA change	Amino acid change
Supp-14 (continued)								
3510969	AA	GC	14	41	34.15	*yvfH*	190_191delAAinsGC	Lys64Ala
3510977	G	A	21	40	52.5	*yvfH*	198G>A	
3510979	T	A	20	40	50	*yvfH*	200T>A	Met67Lys
4214191	G	T	31	31	100	*spoIIIJ*	418C>A	Gln140Lys
Supp-15								
1976137	C	T	134	134	100	*ppsC*	6412G>A	Asp2138Asn
4214191	G	T	49	49	100	*spoIIIJ*	418C>A	Gln140Lys
Supp-16								
4205388	G	A	93	94	98.94	*yyaC*	489G>A	
4214191	G	T	59	59	100	*spoIIIJ*	418C>A	Gln140Lys

*Suppressor 8 is not listed here as it contains over 900 SNPs compared with strain 168, and is possibly a contamination of PY79 endospore that survived genomic DNA extraction.

Table S3. Amino acid substitutions in SpoIIIJ variants selected in *yhdL* depletion strain

Suppressor	Total Charge	T119G (Ile72Arg)	A122G (Gln73Arg)	T131G (Ile76Arg)	C322A (Gln140Lys)	T335G (Leu144Arg)	T586C (Trp228Arg)	G595C (Gly231Arg)
1	3				1	1		1
2	2						1	1
3	2				1	1		
4	2					1		1
5	2						1	1
6	3	1			1	1		
7	3	1			1	1		
8	2	1			1			
9	2		1				1	
10	2	1			1			
11	2		1		1			
12	2				1		1	
13	2	1			1			
14	2			1		1		
15	2			1			1	
16	2				1		1	
17	2				1		1	
18	2						1	1
19	3				1	1		1
20	2		1				1	
21	3			1	1		1	
22	2						1	1
23	2		1				1	
24	2			1			1	
25	2						1	1
26	2				1		1	
27	2	1			1			
28	3			1	1		1	
29	2		1		1			
30	2		1				1	
31	2	1			1			
32	2				1			1
33	3	1			1	1		
34	2						1	1
35	2			1			1	
36	2			1		1		
37	3				1	1		1
38	2				1	1		
39	2			1		1		
40	2		1			1		
41	2				1			1

Suppressor	Total Charge	T119G (Ile72Arg)	A122G (Gln73Arg)	T131G (Ile76Arg)	C322A (Gln140Lys)	T335G (Leu144Arg)	T586C (Trp228Arg)	G595C (Gly231Arg)
42	2		1					1
43	2			1		1		
44	2				1	1		
45	2			1		1		
46	2	1				1		
47	2	1			1			
48	2						1	1
49	2		1		1			
50	2		1				1	
51	2				1		1	
52	2	1			1			
53	2				1		1	
54	2				1		1	
55	2				1		1	
56	2						1	1
57	2				1		1	
58	2				1			1
59	3			1	1		1	
60	2	1				1		
61	2				1		1	
62	2						1	1
63	2				1	1		
64	2			1		1		
65	2		1			1		
66	3			1	1		1	
67	2				1	1		
68	2		1		1			
69	2						1	1
70	2				1	1		
71	2				1	1		
72	2						1	1
73	2				1		1	
74	2		1			1		
75	2				1		1	
76	2				1	1		
77	2				1		1	
78	2				1	1		
79	2				1		1	
80	2				1	1		
81	2			1			1	
82	2	1			1			
83	2				1	1		
84	2	1			1			

Suppressor	Total Charge	T119G (Ile72Arg)	A122G (Gln73Arg)	T131G (Ile76Arg)	C322A (Gln140Lys)	T335G (Leu144Arg)	T586C (Trp228Arg)	G595C (Gly231Arg)
85	2		1				1	
86	2				1	1		
87	2		1				1	
88	2				1	1		
89	2				1	1		
90	2				1		1	
91	2				1	1		
92	2	1			1			
93	2		1		1			
94	2			1		1		
95	3		1		1	1		
96	3			1	1		1	
97	2				1	1		
98	3		1		1	1		
99	2				1	1		
100	2		1		1			
101	2			1		1		
102	2	1				1		
103	3		1		1	1		

Table S4. Secreted and membrane-associated proteins in the σ^M regulon

Locus	Gene	Protein Localization	Number of predicted transmembrane segments
BSU00570	*yabM*	cytoplasmic membrane	14
BSU00600	*yabP*	forespore outer membrane	Unknown
BSU00610	*yabQ*	forespore outer membrane	6
BSU00620	*divIC*	peripheral membrane protein	Peripheral
BSU00690	*ftsH*	cytoplasmic membrane	2
BSU02900	*yceD*	peripheral membrane protein	Peripheral
BSU02920	*yceF*	cytoplasmic membrane	6
BSU03240	*ycgQ*	cytoplasmic membrane	4
BSU03250	*ycgR*	cytoplasmic membrane	8
BSU04230	*amj*	cytoplasmic membrane	7
BSU06380	*yebC*	cytoplasmic membrane	5
BSU09500	*yhdK*	cytoplasmic membrane	3
BSU09510	*yhdL*	cytoplasmic membrane	1
BSU15220	*murG*	peripheral membrane protein	Peripheral
BSU15240	*divIB*	cytoplasmic membrane	1
BSU15250	*ylxW*	Integral membrane protein	Unknown
BSU15260	*ylxX*	cytoplasmic membrane	1
BSU15270	*sbp*	cytoplasmic membrane	3
BSU15280	*ftsA*	cytoplasmic membrane and cytoplasm	Peripheral
BSU15290	*ftsZ*	cytoplasmic membrane and cytoplasm	Peripheral
BSU18190	*yngC*	cytoplasmic membrane	4
BSU21920	*ugtP*	peripheral membrane protein	Peripheral
BSU22320	*ponA*	cytoplasmic membrane	1
BSU27160	*yrhJ*	cytoplasmic membrane	Unknown
BSU27650	*secDF*	cytoplasmic membrane	12
BSU27990	*minD*	peripheral membrane protein	Peripheral
BSU28000	*minC*	peripheral membrane protein	Peripheral
BSU28010	*mreD*	cytoplasmic membrane	5
BSU28020	*mreC*	cytoplasmic membrane	1
BSU28030	*mreB*	peripheral membrane protein	Peripheral
BSU35650	*tagU*	cytoplasmic membrane	1
BSU35840	*tagT*	cytoplasmic membrane	1
BSU36530	*bcrC*	cytoplasmic membrane	4
BSU38120	*rodA*	cytoplasmic membrane	11
BSU38260	*efeB*	Secreted protein	Secreted
BSU38270	*efeO*	cytoplasmic membrane	Peripheral
BSU38280	*efeU*	cytoplasmic membrane	6
BSU38510	*dltB*	cytoplasmic membrane	10

Table S5. *Bacillus subtilis* strains used in this study

Number	Genotype	Note
HB16780	ΔP_M-*murG*	Mutated sigM promoter inside *murG* gene using vector pMutin4
HB16812	ΔP_M-*murG* ΔP_M-*maf*	
HB17934	ΔP_M-*maf*	Mutated sigM promoter inside *maf* gene using vector pMutin4
HB18905	*spx*::P*spx*(P_{M1}*)-*spx* (*kan*)	From Daniel RT(1)
HB20830	*yhdK*::*erm*	All gene::*erm* and gene::*kan* strains were constructed as using genomic DNA of BKE or BKK strains into recipient strains(2)
HB20922	*spx*::P_{spx}(P_{M1}*)-*spx* (*kan*) *yhdK*::*erm*	
HB21099	ΔP_M-*rodA*	P_M promoter of *rodA* removed using CRISPR
HB21117	ΔP_M-*rodA* ΔP_M-*murG*	ΔP_M-*murG* transformed with CRISPR plasmid to remove P_M of *rodA*
HB21118	ΔP_M-*rodA* ΔP_M-*maf*	ΔP_M-*maf* transformed with CRISPR plasmid to remove P_M of *rodA*
HB21266	ΔP_M-*maf* ΔP_M-*murG* ΔP_M-*rodA*	P_M promoter of *rodA* removed using CRISPR from ΔP_M-*maf* ΔP_M-*murG* background
HB25433	ΔP_M-*maf yhdK*::*erm*	
HB25434	ΔP_M-*murG yhdK*::*erm*	
HB25435	ΔP_M-*rodA yhdK*::*erm*	
HB25436	ΔP_M-*murG* ΔP_M-*maf yhdK*::*erm*	
HB25437	ΔP_M-*rodA* ΔP_M-*maf yhdK*::*erm*	
HB25438	ΔP_M-*rodA* ΔP_M-*murG yhdK*::*erm*	
HB25439	ΔP_M-*maf* ΔP_M-*murG* ΔP_M-*rodA yhdK*::*erm*	
HB21248	PY79 P_M-*lacZ yhdL*::*kan*	PY79 background, *yhdL* is not essential in PY79 background
HB21258	168 P_M-*lacZ yhdL*::*kan* congression from PY79-1	
HB21259	168 P_M-*lacZ yhdL*::*kan* congression from PY79-2	
HB21260	168 P_M-*lacZ yhdL*::*kan* congression from PY79-3	
HB21261	168 P_M-*lacZ yhdL*::*kan* congression from PY79-4	
HB21262	168 P_M-*lacZ yhdL*::*kan* congression from PY79-5	
HB21263	168 P_M-*lacZ yhdL*::*kan* congression from PY79-6	
HB21264	168 P_M-*lacZ yhdL*::*kan* congression from PY79-7	
HB21265	168 P_M-*lacZ yhdL*::*kan* congression from PY79-8	Not included in Figure S1, as this strain contains too many SNPs from PY79, possible endospore contamination from PY79 genomic DNA prep
HB21250	168 P_M-*lacZ yhdL*::*kan* congression from PY79-9	
HB21251	168 P_M-*lacZ yhdL*::*kan* congression from PY79-10	

HB21252	168 P_M-*lacZ yhdL*::*kan* congression from PY79-11	
HB21253	168 P_M-*lacZ yhdL*::*kan* congression from PY79-12	
HB21254	168 P_M-*lacZ yhdL*::*kan* congression from PY79-13	
HB21255	168 P_M-*lacZ yhdL*::*kan* congression from PY79-14	
HB21256	168 P_M-*lacZ yhdL*::*kan* congression from PY79-15	
HB21257	168 P_M-*lacZ yhdL*::*kan* congression from PY79-16	
HB22728	*spoIIIJ*	
HB22789	P_M-*lacZ* SpoIIIJ^{Q140K} *yhdL*::*kan*	
HB22848	SpoIIIJ^{Q140K} *yhdK*::*erm*	
HB22849	PY79 P_M-*lacZ* SpoIIIJ^{K140Q} *yhdK*::*erm*	
HB22850	PY79 P_M-*lacZ spoIIIJ yhdK*::*erm*	
HB22883	PY79 *yhdK*::*erm*	
HB22925	PY79 P_M-*lacZ* SpoIIIJ^{K140Q}	
HB22926	PY79 P_M-*lacZ spoIIIJ*	
HB22966	SpoIIIJ^{Q140K}	*spoIIIJ* was mutated at its native locus using CRISPR
HB23553	*amyE*::$P_{spac(hy)}$-*spoIIIJ*	*amyE*::$P_{spac(hy)}$ constructs were made using plasmid pPL82
HB23556	*amyE*::$P_{spac(hy)}$-*yidC2*	
HB23558	*amyE*::$P_{spac(hy)}$-*E.coli-yidC*	
HB23595	*amyE*::$P_{spac(hy)}$-*E.coli*-YidC^{Q429K}	
HB25405	*amyE*::$P_{spac(hy)}$-*spoIIIJ yhdK*::*erm*	
HB25406	*amyE*::$P_{spac(hy)}$-*yidC2 yhdK*::*erm*	
HB25407	*amyE*::$P_{spac(hy)}$-*E.coli-yidC yhdK*::*erm*	
HB25408	*amyE*::$P_{spac(hy)}$-*E.coli*-YidC^{Q429K} *yhdK*::*erm*	
HB23605	*thrC*::P_M-*spoVG-lacZ*-spec *ganA*::P_{xylA}-*yhdL amyE::spoIIIJ yhdL*::*kan*	*ganA*::P_{xylA}-*yhdL* was constructed using pAX01, *thrC*::P_M-*spoVG-lacZ* reporter was constructed using pDG1663, with the *Erm*^{R} cassette replaced by a Spec^R cassette using LFH PCR
HB23606	*thrC*::P_M-*spoVG-lacZ*-spec *ganA*::P_{xylA}-*yhdL amyE::spoIIIJ*-jag *yhdL*::*kan*	
HB23607	*thrC*::P_M-*spoVG-lacZ*-spec *ganA*::P_{xylA}-*yhdL amyE::yidC2 yhdL*::*kan*	
HB23608	*thrC*::P_M-*spoVG-lacZ*-spec *ganA*::P_{xylA}-*yhdL amyE::E.coli-yidC yhdL*::*kan*	
HB23609	*thrC*::P_M-*spoVG-lacZ*-spec *ganA*::P_{xylA}-*yhdL amyE:: E.coli*-YidC^{Q429K} *yhdL*::*kan*	
HB23610	SpoIIIJ^{R73A} *ganA*::P_{xylA}-*yidC2 yidC2*::*kan*	*ganA*::P_{xylA}-*yidC2* was constructed using pAX01
HB23611	SpoIIIJ^{R73AQ140K} *ganA*::P_{xylA}-*yidC2 yidC2*::*kan*	
HB23698	SpoIIIJ^{R73AQ140K} *ganA*::P_{xylA}-*yhdL*-cat *yhdL*::*kan*	*ganA*::P_{xylA}-*yhdL*-cat was constructed using pAX01, and the original *Erm*^{R} cassette in pAX01 was replaced by a CM^R cassette using LFH PCR

HB23719	SpoIIIJ^{Q140K} *ganA*::P_{xylA}-*yhdL*-cat *yhdL*::*Kan*	
HB23902	*amyE*::$P_{spac(hy)}$-YidC2^{Q148K}	
HB25409	*amyE*::$P_{spac(hy)}$- YidC2^{Q148K} *yhdK*::*erm*	
HB23917	*yidC2'-lacZ*	Genomic DNA of SCB751 transformed into 168(3)
HB23918	*yidC2'-lacZ spoIIIJ*	Genomic DNA of SCB751 transformed into HB22728(3)
HB23935	*yidC2'-lacZ spoIIIJ thrC*::*spoIIIJ*-spec	
HB23953	*ganA*::P_{xylA}-*yhdL* P_M-*lacZ yhdL*::*kan*	
HB23955	*yidC2 ganA*::P_{xylA}-*yidC2 spoIIIJ*::*kan*	
HB23965	*thrC*::*spoIIIJ*-spec	*thrC*::*spoIIIJ*-spec WT allele was constructed using LFH PCR
HB23966	P_M-*lacZ thrC*::*spoIIIJ*-spec	
HB23967	*spoIIIJ* P_M-*lacZ thrC*::*spoIIIJ*-spec	
HB23968	*yidC2* P_{xylA}-*yidC2 spoIIIJ*::*kan thrC*::*spoIIIJ*-spec	
HB23969	*thrC*::SpoIIIJ^{Q140K}-spec ΔP_M-*maf*	
HB23970	*thrC*::SpoIIIJ^{Q140K}-spec ΔP_M-*murG*	
HB23971	*thrC*::SpoIIIJ^{Q140K}-spec ΔP_M-*rodA*	
HB23972	*thrC*::SpoIIIJ^{Q140K}-spec ΔP_M-*maf* ΔP_M-*murG*	
HB23973	*thrC*::SpoIIIJ^{Q140K}-spec ΔP_M-*maf* ΔP_M-*rodA*	
HB23974	*thrC*::SpoIIIJ^{Q140K}-spec ΔP_M-*murG* ΔP_M-*rodA*	
HB23975	*thrC*::SpoIIIJ^{Q140K}-spec ΔP_M-*maf* ΔP_M-*murG* ΔP_M-*rodA*	
HB25440	*thrC*::SpoIIIJ^{Q140K}-spec ΔP_M-*maf yhdK*::*erm*	
HB25441	*thrC*::SpoIIIJ^{Q140K}-spec ΔP_M-*murG yhdK*::*erm*	
HB25442	*thrC*::SpoIIIJ^{Q140K}-spec ΔP_M-*rodA yhdK*::*erm*	
HB25443	*thrC*::SpoIIIJ^{Q140K}-spec ΔP_M-*maf* ΔP_M-*murG yhdK*::*erm*	
HB25444	*thrC*::SpoIIIJ^{Q140K}-spec ΔP_M-*maf* ΔP_M-*rodA yhdK*::*erm*	
HB25445	*thrC*::SpoIIIJ^{Q140K}-spec ΔP_M-*murG* ΔP_M-*rodA yhdK*::*erm*	
HB25446	*thrC*::SpoIIIJ^{Q140K}-spec ΔP_M-*maf* ΔP_M-*murG* ΔP_M-*rodA yhdK*::*erm*	
HB23976	*thrC*::*spoIIIJ*-spec WT (R73)	
HB23977	P_M-*lacZ thrC*::*spoIIIJ*-spec WT (R73)	
HB23978	*spoIIIJ* P_M-*lacZ thrC*::*spoIIIJ*-spec WT (R73)	
HB25354	*spoIIIJ* P_M-*lacZ thrC*::*spoIIIJ*-spec sup (R144R231)	*thrC*::*spoIIIJ*-spec allele variants were constructed using degenerative primers and LFH PCR
HB25355	*spoIIIJ* P_M-*lacZ thrC*::*spoIIIJ*-spec sup (R72K140)	
HB25356	*spoIIIJ* P_M-*lacZ thrC*::*spoIIIJ*-spec sup (R73R228)	

HB25357	*spoIIIJ* P_M-*lacZ thrC*::*spoIIIJ*-spec sup (K140R231)
HB25358	*spoIIIJ* P_M-*lacZ thrC*::*spoIIIJ*-spec sup (R76R144)
HB25359	*spoIIIJ* P_M-*lacZ thrC*::*spoIIIJ*-spec sup (R73R144)
HB25360	*spoIIIJ* P_M-*lacZ thrC*::*spoIIIJ*-spec sup (R73R231)
HB25361	*spoIIIJ* P_M-*lacZ thrC*::*spoIIIJ*-spec sup (K140R228)
HB25362	*spoIIIJ* P_M-*lacZ thrC*::*spoIIIJ*-spec sup (R228R231)
HB25363	*spoIIIJ* P_M-*lacZ thrC*::*spoIIIJ*-spec sup (R72R144)
HB25364	*spoIIIJ* P_M-*lacZ thrC*::*spoIIIJ*-spec sup (K140R144R231)
HB25366	*spoIIIJ* P_M-*lacZ thrC*::*spoIIIJ*-spec sup (R73K140R144)
HB25376	*yhdK*::*erm spoIIIJ* P_M-*lacZ thrC*::*spoIIIJ*-spec sup (R144R231)
HB25377	*yhdK*::*erm spoIIIJ* P_M-*lacZ thrC*::*spoIIIJ*-spec sup (R72K140)
HB25378	*yhdK*::*erm spoIIIJ* P_M-*lacZ thrC*::*spoIIIJ*-spec sup (R73R228)
HB25379	*yhdK*::*erm spoIIIJ* P_M-*lacZ thrC*::*spoIIIJ*-spec sup (K140R231)
HB25380	*yhdK*::*erm spoIIIJ* P_M-*lacZ thrC*::*spoIIIJ*-spec sup (R76R144)
HB25381	*yhdK*::*erm spoIIIJ* P_M-*lacZ thrC*::*spoIIIJ*-spec sup (R73R144)
HB25382	*yhdK*::*erm spoIIIJ* P_M-*lacZ thrC*::*spoIIIJ*-spec sup (R73R231)
HB25383	*yhdK*::*erm spoIIIJ* P_M-*lacZ thrC*::*spoIIIJ*-spec sup (K140R228)
HB25384	*yhdK*::*erm spoIIIJ* P_M-*lacZ thrC*::*spoIIIJ*-spec sup (R228R231)
HB25385	*yhdK*::*erm spoIIIJ* P_M-*lacZ thrC*::*spoIIIJ*-spec sup (R72R144)
HB25386	*yhdK*::*erm spoIIIJ* P_M-*lacZ thrC*::*spoIIIJ*-spec sup (K140R144R231)
HB25387	*yhdK*::*erm spoIIIJ* P_M-*lacZ thrC*::*spoIIIJ*-spec sup (R73K140R144)
HB23987	*spoIIIJ* P_M-*lacZ thrC*::*spoIIIJ*-spec sup (R73K140)
HB23988	*spoIIIJ* P_M-*lacZ thrC*::*spoIIIJ*-spec sup (R76R228)
HB23989	*spoIIIJ* P_M-*lacZ thrC*::*spoIIIJ*-spec sup (K140R144)
HB23990	*spoIIIJ* P_M-*lacZ thrC*::*spoIIIJ*-spec sup (R72K140R144)
HB23991	*spoIIIJ* P_M-*lacZ thrC*::*spoIIIJ*-spec sup (R76K140R228)
HB25388	*yhdK*::*erm spoIIIJ* P_M-*lacZ thrC*::*spoIIIJ*-spec sup (R73K140)
HB25389	*yhdK*::*erm spoIIIJ* P_M-*lacZ thrC*::*spoIIIJ*-spec sup (R76R228)
HB25390	*yhdK*::*erm spoIIIJ* P_M-*lacZ thrC*::*spoIIIJ*-spec sup (K140R144)
HB25391	*yhdK*::*erm spoIIIJ* P_M-*lacZ thrC*::*spoIIIJ*-spec sup (R72K140R144)
HB25392	*yhdK*::*erm spoIIIJ* P_M-*lacZ thrC*::*spoIIIJ*-spec sup (R76K140R228)
HB25404	*yhdK*::*erm spoIIIJ* P_M-*lacZ thrC*::*spoIIIJ*-spec WT (R73)

HB25107	P_M-*lacZ ganA*::P_{xylA}-*yhdL yhdL*::*kan spoIIIJ thrC*::*spoIIIJ* sup (R144R231)
HB25108	P_M-*lacZ ganA*::P_{xylA}-*yhdL yhdL*::*kan spoIIIJ thrC*::*spoIIIJ* sup (R72K140)
HB25109	P_M-*lacZ ganA*::P_{xylA}-*yhdL yhdL*::*kan spoIIIJ thrC*::*spoIIIJ* sup (R73K140)
HB25110	P_M-*lacZ ganA*::P_{xylA}-*yhdL yhdL*::*kan spoIIIJ thrC*::*spoIIIJ* sup (R73R228)
HB25111	P_M-*lacZ ganA*::P_{xylA}-*yhdL yhdL*::*kan spoIIIJ thrC*::*spoIIIJ* sup (R76R228)
HB25112	P_M-*lacZ ganA*::P_{xylA}-*yhdL yhdL*::*kan spoIIIJ thrC*::*spoIIIJ* sup (K140R231)
HB25113	P_M-*lacZ ganA*::P_{xylA}-*yhdL yhdL*::*kan spoIIIJ thrC*::*spoIIIJ* sup (R76R144)
HB25114	P_M-*lacZ ganA*::P_{xylA}-*yhdL yhdL*::*kan spoIIIJ thrC*::*spoIIIJ* sup (K140R144)
HB25115	P_M-*lacZ ganA*::P_{xylA}-*yhdL yhdL*::*kan spoIIIJ thrC*::*spoIIIJ* sup (R73R144)
HB25116	P_M-*lacZ ganA*::P_{xylA}-*yhdL yhdL*::*kan spoIIIJ thrC*::*spoIIIJ* sup (R73R231)
HB25117	P_M-*lacZ ganA*::P_{xylA}-*yhdL yhdL*::*kan spoIIIJ thrC*::*spoIIIJ* sup (K140R228)
HB25118	P_M-*lacZ ganA*::P_{xylA}-*yhdL yhdL*::*kan spoIIIJ thrC*::*spoIIIJ* sup (R228R231)
HB25119	P_M-*lacZ ganA*::P_{xylA}-*yhdL yhdL*::*kan spoIIIJ thrC*::*spoIIIJ* sup (R72R144)
HB25120	P_M-*lacZ ganA*::P_{xylA}-*yhdL yhdL*::*kan spoIIIJ thrC*::*spoIIIJ* sup (R72K140R144)
HB25121	P_M-*lacZ ganA*::P_{xylA}-*yhdL yhdL*::*kan spoIIIJ thrC*::*spoIIIJ* sup (R76K140R228)
HB25122	P_M-*lacZ ganA*::P_{xylA}-*yhdL yhdL*::*kan spoIIIJ thrC*::*spoIIIJ* sup (K140R144R231)
HB25123	P_M-*lacZ ganA*::P_{xylA}-*yhdL yhdL*::*kan spoIIIJ thrC*::*spoIIIJ* sup (R73K140R228)
HB25124	P_M-*lacZ ganA*::P_{xylA}-*yhdL yhdL*::*kan spoIIIJ thrC*::*spoIIIJ* sup (R73K140R144)
HB25227	*yidC2*'-*lacZ spoIIIJ thrC*::*spoIIIJ* sup (R144R231)
HB25228	*yidC2*'-*lacZ spoIIIJ thrC*::*spoIIIJ* sup (R72K140)
HB25229	*yidC2*'-*lacZ spoIIIJ thrC*::*spoIIIJ* sup (R73K140)
HB25230	*yidC2*'-*lacZ spoIIIJ thrC*::*spoIIIJ* sup (R73R228)
HB25231	*yidC2*'-*lacZ spoIIIJ thrC*::*spoIIIJ* sup (R76R228)
HB25232	*yidC2*'-*lacZ spoIIIJ thrC*::*spoIIIJ* sup (K140R231)
HB25233	*yidC2*'-*lacZ spoIIIJ thrC*::*spoIIIJ* sup (R76R144)
HB25234	*yidC2*'-*lacZ spoIIIJ thrC*::*spoIIIJ* sup (K140R144)
HB25235	*yidC2*'-*lacZ spoIIIJ thrC*::*spoIIIJ* sup (R73R144)
HB25236	*yidC2*'-*lacZ spoIIIJ thrC*::*spoIIIJ* sup (R73R231)
HB25237	*yidC2*'-*lacZ spoIIIJ thrC*::*spoIIIJ* sup (K140R228)
HB25238	*yidC2*'-*lacZ spoIIIJ thrC*::*spoIIIJ* sup (R228R231)
HB25239	*yidC2*'-*lacZ spoIIIJ thrC*::*spoIIIJ* sup (R72R144)
HB25240	*yidC2*'-*lacZ spoIIIJ thrC*::*spoIIIJ* sup (R72K140R144)

HB25241	*yidC2'-lacZ spoIIIJ thrC*::*spoIIIJ* sup (R76K140R228)
HB25242	*yidC2'-lacZ spoIIIJ thrC*::*spoIIIJ* sup (K140R144R231)
HB25243	*yidC2'-lacZ spoIIIJ thrC*::*spoIIIJ* sup (R73K140R228)
HB25244	*yidC2'-lacZ spoIIIJ thrC*::*spoIIIJ* sup (R73K140R144)
HB25287	*yidC2 ganA*::P_{xylA}-*yidC2 spoIIIJ*::*kan thrC*::*spoIIIJ* sup (R144R231)
HB25288	*yidC2 ganA*::P_{xylA}-*yidC2 spoIIIJ*::*kan thrC*::*spoIIIJ* sup (R72K140)
HB25289	*yidC2 ganA*::P_{xylA}-*yidC2 spoIIIJ*::*kan thrC*::*spoIIIJ* sup (R73K140)
HB25290	*yidC2 ganA*::P_{xylA}-*yidC2 spoIIIJ*::*kan thrC*::*spoIIIJ* sup (R73R228)
HB25291	*yidC2 ganA*::P_{xylA}-*yidC2 spoIIIJ*::*kan thrC*::*spoIIIJ* sup (R76R228)
HB25292	*yidC2 ganA*::P_{xylA}-*yidC2 spoIIIJ*::*kan thrC*::*spoIIIJ* sup (K140R231)
HB25293	*yidC2 ganA*::P_{xylA}-*yidC2 spoIIIJ*::*kan thrC*::*spoIIIJ* sup (R76R144)
HB25294	*yidC2 ganA*::P_{xylA}-*yidC2 spoIIIJ*::*kan thrC*::*spoIIIJ* sup (K140R144)
HB25295	*yidC2 ganA*::P_{xylA}-*yidC2 spoIIIJ*::*kan thrC*::*spoIIIJ* sup (R73R144)
HB25296	*yidC2 ganA*::P_{xylA}-*yidC2 spoIIIJ*::*kan thrC*::*spoIIIJ* sup (R73R231)
HB25297	*yidC2 ganA*::P_{xylA}-*yidC2 spoIIIJ*::*kan thrC*::*spoIIIJ* sup (K140R228)
HB25298	*yidC2 ganA*::P_{xylA}-*yidC2 spoIIIJ*::*kan thrC*::*spoIIIJ* sup (R228R231)
HB25299	*yidC2 ganA*::P_{xylA}-*yidC2 spoIIIJ*::*kan thrC*::*spoIIIJ* sup (R72R144)
HB25300	*yidC2 ganA*::P_{xylA}-*yidC2 spoIIIJ*::*kan thrC*::*spoIIIJ* sup (R72K140R144)
HB25301	*yidC2 ganA*::P_{xylA}-*yidC2 spoIIIJ*::*kan thrC*::*spoIIIJ* sup (R76K140R228)
HB25302	*yidC2 ganA*::P_{xylA}-*yidC2 spoIIIJ*::*kan thrC*::*spoIIIJ* sup (K140R144R231)
HB25303	*yidC2 ganA*::P_{xylA}-*yidC2 spoIIIJ*::*kan thrC*::*spoIIIJ* sup (R73K140R228)
HB25304	*yidC2 ganA*::P_{xylA}-*yidC2 spoIIIJ*::*kan thrC*::*spoIIIJ* sup (R73K140R144)
HB23636	*htrA*::*kan*
HB23637	*htrB*::*kan*
HB23638	*glpG*::*kan*
HB23639	*sipS*::*kan*
HB23640	*sipT*::*kan*
HB23641	*htpX*::*kan*
HB23648	*htrAB*
HB23650	P_{htrA}-*lux*
HB23651	*cssR*
HB23653	*cssS*

HB23657	P_{htrA}-*lux spoIIIJ*^{Q140K}	
HB23660	*amyE*::$P_{spac(hy)}$-none	pPL82 empty vector
HB23663	*amyE*::$P_{spac(hy)}$-*htrA*	constructed using pPL82
HB23664	*amyE*::$P_{spac(hy)}$-*htrB*	constructed using pPL82
HB23667	P_{htrA}-*lux cssR*::*kan*	
HB23668	P_{htrA}-*lux cssS*::*kan*	
HB23682	*prsW*::*kan*	
HB23690	*cssS htrB*	
HB23910	*secDF*	
HB23926	*sasA*	
HB23806	*bshC*	
HB23807	*msrA*	
HB23808	*nfrA*	
HB23809	*tpx*	
HB23811	*bshA*	
HB25410	*htrA*::*kan yhdK*::*erm*	
HB25411	*htrB*::*kan yhdK*::*erm*	
HB25412	*glpG*::*kan yhdK*::*erm*	
HB25413	*sipS*::*kan yhdK*::*erm*	
HB25414	*sipT*::*kan yhdK*::*erm*	
HB25415	*htpX*::*kan yhdK*::*erm*	
HB25416	*htrAB yhdK*::*erm*	
HB25417	*cssR yhdK*::*erm*	
HB25418	*cssS yhdK*::*erm*	
HB25419	*prsW*::*kan yhdK*::*erm*	
HB25420	*cssS htrB yhdK*::*erm*	
HB25421	*secDF yhdK*::*erm*	
HB25422	*sasA yhdK*::*erm*	
HB25423	*bshC yhdK*::*erm*	
HB25424	*msrA yhdK*::*erm*	
HB25425	*nfrA yhdK*::*erm*	
HB25426	*tpx yhdK*::*erm*	

HB25427	*bshA yhdK*::*erm*
HB25428	*amyE*::$P_{spac(hy)}$-none *yhdK*::*erm*
HB25429	*amyE*::$P_{spac(hy)}$-*htrA yhdK*::*erm*
HB25430	*amyE*::$P_{spac(hy)}$-*htrB yhdK*::*erm*
HB25431	P_{htrA}-*lux yhdK*::*erm*
HB25432	P_{htrA}-*lux spoIIIJ*^{Q140K} *yhdK*::*erm*

Table S6. Primers used in this study

Number	Name	Sequence
1295	kan-F	CAGCGAACCATTTGAGGTGATAGG
1296	kan-R	CGATACAAATTCCTCGTAGGCGCTCG
6580	sigM-F-NotI	ATCGGCGGCCGCGCACTATCTTTTGCGGCCAT
6581	sigM-R-HindIII	ATCGAAGCTTTGGTCGCTCATTTCCCCATT
6582	yhdL-up-F	GCCGTTTTCGTTGCGAGAAT
6583	yhdL-up-R	CGCCGACATTCGCTGATTTTTCCTGGTCGCTCATTTCCC
6584	yhdL-mid-F	GGGAAATGAGCGACCAGGAAAAATCAGCGAATGTCGGCG
6585	yhdL-mid-R	CCTATCACCTCAAATGGTTCGCTGTCCGAAAACCGGTATAACGAAA
6586	yhdL-down-F	CGAGCGCCTACGAGGAATTTGTATCGAGATACGAATTTACAGTTTGGCT
6587	yhdL-down-R	ACGAATCGGGCAATCATGTG
6588	chr-sigM-seq-F	CCATTGTGCCACTCCTTCAC
6589	chr-sigM-seq-R	TGCAGTCATTTCCTGGTCGC
6590	pAX01-check-F	GGGGGAAATGACAAATGGTCC
6591	pAX01-check-R	ACGAAAGGGCCTCGTGATAC
6599	Pxyl-yhdL-F-BamHI	ATCGGGATCCTAGAGGGGAGAAAAGGCAATGATGAATGAAGAATTTAAAAAGC
6600	Pxyl-yhdL-R-SacII	ATCGCCGCGGTCCAGCCGAATACATTGTG
6693	pAX01-erm-cm-up-F	GCCGCACTCTTCCTTTTTCAA
6694	pAX01-erm-cm-up-R	CTTGATAATAAGGGTAACTATTGCCTTTGGTTGAGTACTTTTTCACTCG
6695	pAX01-erm-cm-down-F	GGGTAACTAGCCTCGCCGGTCCACGCTGGGGGAGGAAATAATTCTATGAGTCGC
6696	pAX01-erm-cm-down-R	TCGGCATTTTTGCATGGAGC

6759	yhdL-check-F	ACGCTGGGAAGCTACCTCTA
6760	yhdL-check-R	TCTGCTTTTGCGGTCGTTTG
6808	PsigM-F-EcoRI	AGCTGAATTCGCCGTTTGCATGTAATGTG
6809	PsigM-R-PstI	AGCTCTGCAGCAGTAAGTCTTCAGCAAGATGC
6814	pBs1ClacZ(lux)-check-F	AAAGGATTTGAGCGTAGCGA
6815	pBs1ClacZ-check-R	TTGGGTAACGCCAGGGTTTT
6816	pBs3Clux-check-R	GAGAGTCCTCCTGTCGACCT
6861	cssS-check-F	CCGCGAGGTCTATGACGAAA
6862	cssS-check-R	AGCTCAAGCGAAAGGGTGAA
7348	pJOE8999-check-F	CCTTTTTGCGTGTGATGCGA
7349	pJOE8999-check-R	GTCAGCTAGGAGGTGACTGA
7426	Delta-Pam-rodA-up-F	AAGGCCAACGAGGCCTCTGCTGAACACAGTCACTT
7427	Delta-Pm-rodA-up-R	CGCTTTTTCAGCTACACGAAATGCGATAATGTGTTATGTTCCC
7428	Delta-Pm-rodA-down-F	GGGAACATAACACATTATCGCATTTCGTGTAGCTGAAAAAGCG
7429	Delta-Pm-rodA-down-R	AAGGCCTTATTGGCCCTCATTTGAAGCAGACACCC
7430	ProdA-deltaPm-gRNA-F	TACGCGTTTTTTAACAAATTCTAT
7431	ProdA-deltaPm-gRNA-R	AAACATAGAATTTGTTAAAAAACG
7815	spoIIIJ-seq-F	ACGGGAGATAACTACGGGCT
7816	spoIIIJ-seq-R	GCTTCATCGACATTTCGCCC
7866	spoIIIJ-gRNA-F	TACGATCCAATTAAAATCGGCATC
7867	spoIIIJ-gRNA-R	AAACGATGCCGATTTTAATTGGAT
7868	spoIIIJ-up-F	AAGGCCAACGAGGCCTATTGCCAGAAAACCGGCGA
7869	spoIIIJ-up-R	TCGCATGATAGAATCCAATTAAGATAGGCATCTTGATCAAAATCGGGAAACATCCC
7870	spoIIIJ-down-F	GGGATGTTTCCCGATTTTGATCAAGATGCCTATCTTAATTGGATTCTATCATGCGA
7871	spoIIIJ-down-R	AAGGCCTTATTGGCCATCAGACTTCCCGGCAATGG
8120	yidC2-check-F	TCCTGCTCTAACGGCAATCG
8121	yidC2-check-R	CTTTTTGCACGGGGTTGCTT
8246	spoIIIJ-PY79-to-168-down-F	CATTGGCGGGATGTTTCCCGATCTTGATCCAGATGCCGATTTTAATTGGA
8247	spoIIIJ-PY79-to-168-up-R	AAAATCGGCATCTGGATCAAGATCGGGAAACATCCCGCCAATG
8248	spoIIIJ-PY79-to-168-gRNA-F	TACGATCGGCATCTTGATCAAAAT
8249	spoIIIJ-PY79-to-168-gRNA-R	AAACATTTTGATCAAGATGCCGAT
8250	jag-check-F	TGCGATCATGAGAACCCAGG

8251	jag-check-R	AGTTTGGTTCGAAGTGGAAGA
8264	PsigM-F-HindIII	ATCGAAGCTTGCCGTTTGCATGTAATGTG
8265	PsigM-R-BamHI	ATCGGGATCCCAGTAAGTCTTCAGCAAGATGC
8266	pDG1663-check-F	CCAACATGACGAATCCCTCC
8267	pDG1663-check-R	TAAGTTGGGTAACGCCAGGG
8276	YidC2-SpeI-F	ATCGACTAGTACCGCATTTATAAAAAGGAGGAGAA
8277	YidC2-BamHI-R	ATCGGGATCCTCAGCCATGATAAACAAGACT
8278	spoIIIJ-R73A-gRNA-F	TACGAATTAATAAACGAATTAAAA
8279	spoIIIJ-R73A-gRNA-R	AAACTTTTAATTCGTTTATTAATT
8280	SpoIIIJ-R73A-repair-up-R	GCTGCTTAATCATCAGCGGTAAAATTAATAATGCAATTAAAATGGTAACTAGAATAATTGAAAGC
8281	SpoIIIJ-R73A-repair-down-F	GCTTTCAATTATTCTAGTTACCATTTTAATTGCATTATTAATTTTACCGCTGATGATTAAGCAGC
8282	spoIIIJ-SpeI-F	ATCGACTAGTAGATTAATTATAGGAGGAAATGTTGT
8283	spoIIIJ-BamHI-R	ATCGGGATCCAGCAGTCACATTCCTCACTTTT
8341	Ec-YidC-seq-F	CCACGCCTGACGAGAAGTAT
8342	Ec-YidC-seq-R	AGTTTGAACAGCGGCTGAGA
8343	Ec-YidC-HindIII-F	ATCGAAGCTTTAAGGAGGACTAACGATGGATTCGCAACGCA
8344	Ec-YidC-XbaI-R	ATCGTCTAGAAGCGAAAACTCACCGAATCAGGA
8345	YidC2-HindIII-F	ATCGAAGCTTACCGCATTTATAAAAAGGAGGAGAA
8346	YidC2-XbaI-R	ATCGTCTAGATCAGCCATGATAAACAAGACT
8347	spoIIIJ-XmaI-F	ATCGCCCGGGAGATTAATTATAGGAGGAAATGTTGT
8348	SpoIIIJ-XbaI-R	ATCGTCTAGAAGCAGTCACATTCCTCACTTTT
8349	jag-XbaI-R	ATCGTCTAGAAGTTTGGTTCGAAGTGGAAGA
8352	pDG1663-up-F	TTGGGTAACGCCAGGGTTTT
8353	pDG1663-spec-up-R	CGTTACGTTATTAGCGAGCCAGTCTGGTTGAGTACTTTTTCATTCGTT
8354	pDG1663-spec-down-F	CAATAAACCCTTGCCCTCGCTACGTCAAGCAATGAAACACGCCA
8355	pDG1663-down-R	ACCGCTGTGTTCGGATCTTT
8364	Ec-YidC-Q429K-up-R	AGGAAGATTGGCATCTTGATCAGCAGCGGGAAGCA
8365	Ec-YidC-Q429K-down-F	CTTCCCGCTGCTGATCAAGATGCCAATCTTCCTGGCGT
8371	htrA-check-F	CTGTTCCATCGACTCAGTCCT
8372	htrA-check-R	CGCAGATCATACCCAGTCCC
8373	htrB-check-F	AGAGCGAGGAAGATGTAGGA
8374	htrB-check-R	TCGGCCTGGCTGAAGAAAAT

8375	htpX-check-F	CGCACCATATCGGTTCGAGA
8376	htpX-check-R	AACGGCCACAGTAACTGCAA
8377	sipT-check-F	AGTATCGTGATCGGTGCTGT
8378	sipT-check-R	AAGCGCGGAAAAGAGAACAAA
8379	sipS-check-F	AGGCATGATGTGGGTAGAAGA
8380	sipS-check-R	ACGATGCATAACGGGAATATGT
8381	prsW-check-F	GGCATATCGCAGCGGAAATC
8382	prsW-check-R	TTCAAGCCTCCTACTGCAAA
8383	cssR-check-F	TCCTCGCTCTTTTTCTCTTCCT
8384	cssR-check-R	AGGCGGTACTCTGTCAGAAC
8385	cssR-RT-F	AGGCGAAAGATCCTGACGTG
8386	cssR-RT-R	CTCACGAGAGTATGGATGCCC
8389	cssS-int-F	TTATCGGGACGATTTGGCCT
8390	cssS-int-R	CTCTGATGACCATGACCGGC
8399	htrA-HindIII-F	ATCGAAGCTTTAAGGAGGGAACATGATGGATAACTATCGTGA
8400	htrA-XmaI-R	ATCGCCCGGGTTTACGGCCTGAGGCATTAT
8401	htrB-XmaI-F	ATCGCCCGGGTAAGGAGGTAAGAACATGGATTATCGACGTGA
8402	htrB-XbaI-R	ATCGTCTAGAATGCTTTCCTCTTATTTAGGGTAACA
8403	PhtrA-XbaI-F	ATCGTCTAGATCAACAGCTGTCTAGCGAT
8404	PhtrA-PstI-R	ATCGCTGCAGTCTCTATTTTCACATGTCTATTTATATTGA
8442	htrA-int-F	GCAACAAGCACCTCCTCTGA
8443	htrA-int-R	GTCCACGCCGCTTACAATTC
8444	htrB-int-F	ACGAACGCATCAAACATCGC
8445	htrB-int-R	TGTCAATCATCTGCACGCCT
8652	bshC-check-F	TGCTGGTTGACGTCATTGGA
8653	bshC-check-R	TGCTCACCTAGGCCTTCTCT
8654	msrA-check-F	TGAATTCATTCCGCGACAGC
8655	msrA-check-R	CCGTGCCGTTATTTTGCGTT
8656	nfrA-check-F	GTCAGCTATGGGGGAAGCTC
8657	nfrA-check-R	GTTTCTGCATTGCTGCCCTC
8658	tpx-check-F	TTGTCGGATCGACAGGCATC
8659	tpx-check-R	CACCGCACCTACATGGTCTT

8676	cssS-int-F	TTATCGGGACGATTTGGCCT
8677	cssS-int-R	CTCTGATGACCATGACCGGC
8681	spoIIIJ-spc-2-R	CTCTTGCCAGTCACGTTACGTTATTAGCTGCAGCAGTCACATTCCTCA
8682	spoIIIJ-spc-3-F	TGAGGAATGTGACTGCTGCAGCTAATAACGTAACGTGACTGGCAAGAG
8686	spoIIIJ-MUT-2-F	ATTACCGCTGATGATTAAGCAGCT
8687	spoIIIJ-MUT-3-F	TATTGGATTCTATCATGCGATCAT
8688	spoIIIJ-MUT-4-F	GTAACTTGTTTATGATTGCGCAAACT
8689	spoIIIJ-MUT-1-R	AGCTGCTTAATCATCAGCGGTAATMTTAATAATYGTMTTAAAATGGTAACTAGAATAATT
8690	spoIIIJ-MUT-2-R	ATGATCGCATGATAGAATCCAATAMGAATCGGCATTTKGATCAAAATCGGGAAACATCCC
8691	spoIIIJ-MUT-3-R	AGTTTGCGCAATCATAAACAAGTTACSAACTACCCRATAAAGAGAAAGAGCCGCCGGGAA
8700	dinB-RT-F	CGGCTGGATTGAAGTGTTTT
8701	dinB-RT-R	TGTTTTCATGATTCCGCTTG
8702	lexA-RT-F	GTTCCTCCAGACGAGCATGT
8703	lexA-RT-R	CAAGCGAATGTGGGTATCCT
8712	recA-RT-F	GTTCGGCAAAGGTTCCATTA
8713	recA-RT-R	GCCAATTCCCAGTGCTGTAT
8722	topA-RT-F	CAGCTGACCCCGACAGAGAA
8723	topA-RT-R	ATACGTCTCGCTTGCTGTGC
8726	gyrA-RT-F	GGCGGCCATGCGTTATACAG
8727	gyrA-RT-R	GCCATACCTACCGCAATGCC
8728	gyrB-RT-F	GTGTAGGTGCGTCGGTCGTA
8729	gyrB-RT-R	GCTAATTCACGCACGCGGTT
8736	secG-RT-F	GTGCCGGATTATCTGGTGCG
8737	secG-RT-R	AAGACTGCCAGCACTACCGT
8759	secDF-check-F	GAAGAGGGCCAGGAAGCATT
8760	secDF-check-R	CATTTGCCTTGCTTCAGCGT
8766	thrC-up-1-F	TATGCATCAGGTCGGCTGTC
8767	thrC-spoIIIJ-1-R	TAAGAAAGCAGTGGTGATGCCAGGATTGACGCCTTCCGTTT
8768	thrC-spoIIIJ-2-F	AAACGGAAGGCGTCAATCCTGGCATCACCACTGCTTTCTTA
8769	spec-thrC-3-R	GCAAACACGCCTTCTACACGGCAAGGGTTTATTGTTTTCTAAAATCTG
8770	spec-thrC-down-4-F	CAGATTTTAGAAAACAATAAACCCTTGCCGTGTAGAAGGCGTGTTTGC
8771	thrC-down-4-R	TTCCCCCTCTCCCAAACTGA

8772	thrC-spoIIIJ-check-F	GATCAAACACCGGCGCTAAC
8773	thrC-spoIIIJ-check-R	CAACTCCTGATCCAAACATGTAAGT
8774	spoIIIJ-MUT-seq-F	GATAGTCCGCATTTCTGGGA
8775	spoIIIJ-MUT-seq-R	TCTTGCCAGTCACGTTACGT

1. Rojas-Tapias DF & Helmann JD (2018) Induction of the Spx regulon by cell wall stress reveals novel regulatory mechanisms in Bacillus subtilis. *Mol Microbiol* 107(5):659-674.
2. Koo BM*, et al.* (2017) Construction and Analysis of Two Genome-Scale Deletion Libraries for Bacillus subtilis. *Cell Syst* 4(3):291-305 e297.
3. Chiba S, Lamsa A, & Pogliano K (2009) A ribosome-nascent chain sensor of membrane protein biogenesis in Bacillus subtilis. *EMBO J* 28(22):3461-3475.